
Supplementary Material for “Bias Reduction of Maximum Likelihood Estimates for an Asymmetric Class of Power Models with Applications”

Authors: YOLANDA M. GÓMEZ 

– Departamento de Estadística, Facultad de Ciencias,
Universidad del Bío-Bío, Concepción 4081112, Chile
ygomez@ubiobio.cl

BRUNO SANTOS 

– School of Mathematics Statistics and Actuarial Science,
University of Kent, Canterbury, England
b.santos@kent.ac.uk

DIEGO I. GALLARDO 

– Departamento de Estadística, Facultad de Ciencias,
Universidad del Bío-Bío, Concepción 4081112, Chile
dgallardo@ubiobio.cl

OSVALDO VENEGAS  

– Departamento de Ciencias Matemáticas y Físicas, Facultad de Ingeniería,
Universidad Católica de Temuco, Temuco, Chile
ovenegas@uct.cl

HÉCTOR W. GÓMEZ 

– Departamento de Estadística y Ciencias de Datos, Facultad de Ciencias Básicas,
Universidad de Antofagasta, Antofagasta, Chile
hector.gomez@uantof.cl

Received: November 2020

Revised: February 2022

Accepted: February 2022

This supplementary material contains additional information for the simulation studies discussed in Section 4. We also include two additional real data applications related to the power half-normal (PHN) and the power Birnbaum-Saunders (PBS) distributions.

1. ADDITIONAL MATERIAL FOR THE SIMULATION STUDY

In this Section, we present additional results for the simulation study discussed in Section 4 of the manuscript. The material is related to the extended exponential (EE), PHN and power piecewise exponential (PPE) distributions.

1.1. EE distribution

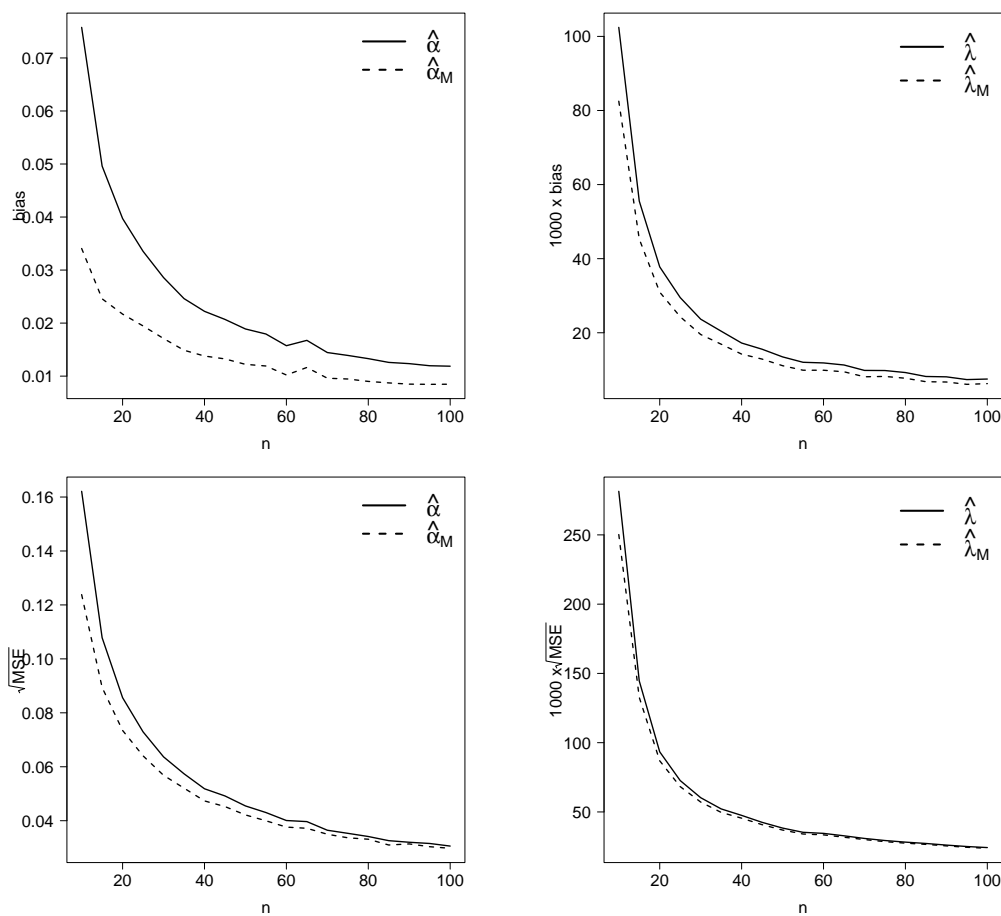


Figure 1: Estimated bias and root MSE for the MLEs and the modified MLEs in the EE($\alpha = 0.25, \lambda = 0.1$) model under different scenarios based on 10,000 replicates.

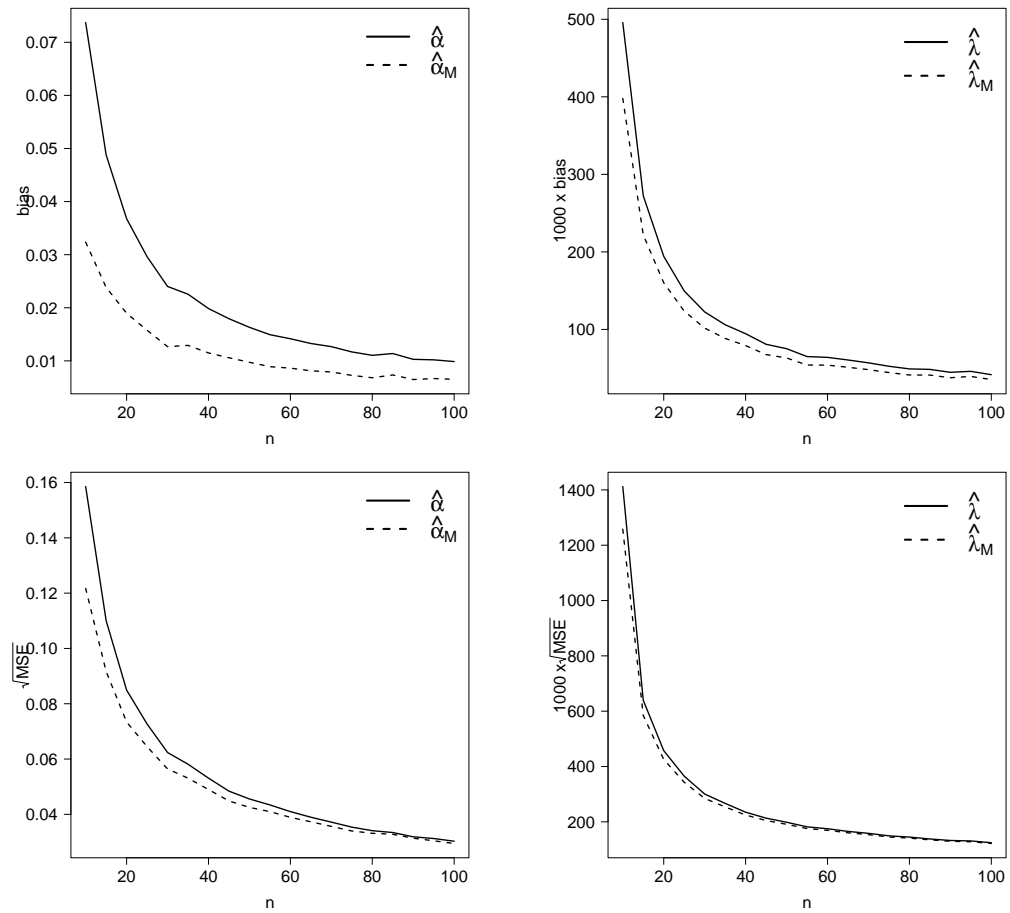


Figure 2: Estimated bias and root MSE for the MLEs and the modified MLEs in the $EE(\alpha = 0.25, \lambda = 0.5)$ model under different scenarios based on 10,000 replicates.

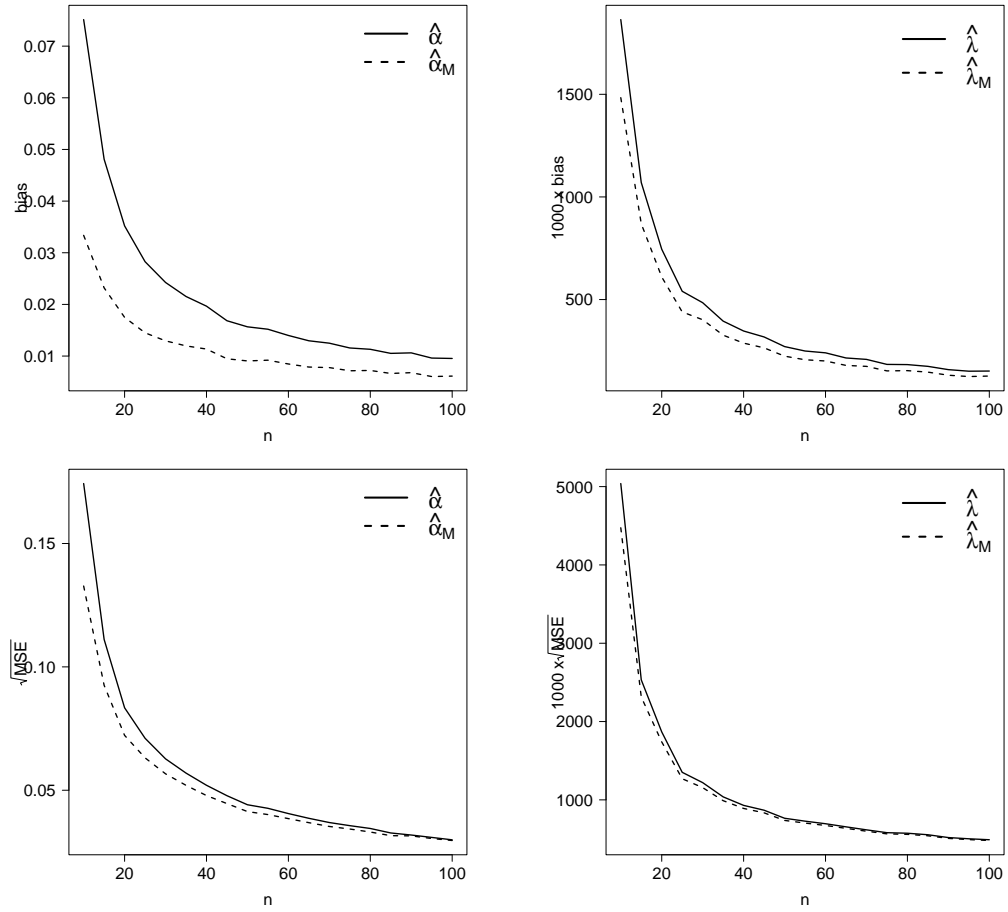


Figure 3: Estimated bias and root MSE for the MLEs and the modified MLEs in the EE($\alpha = 0.25, \lambda = 2$) model under different scenarios based on 10,000 replicates.

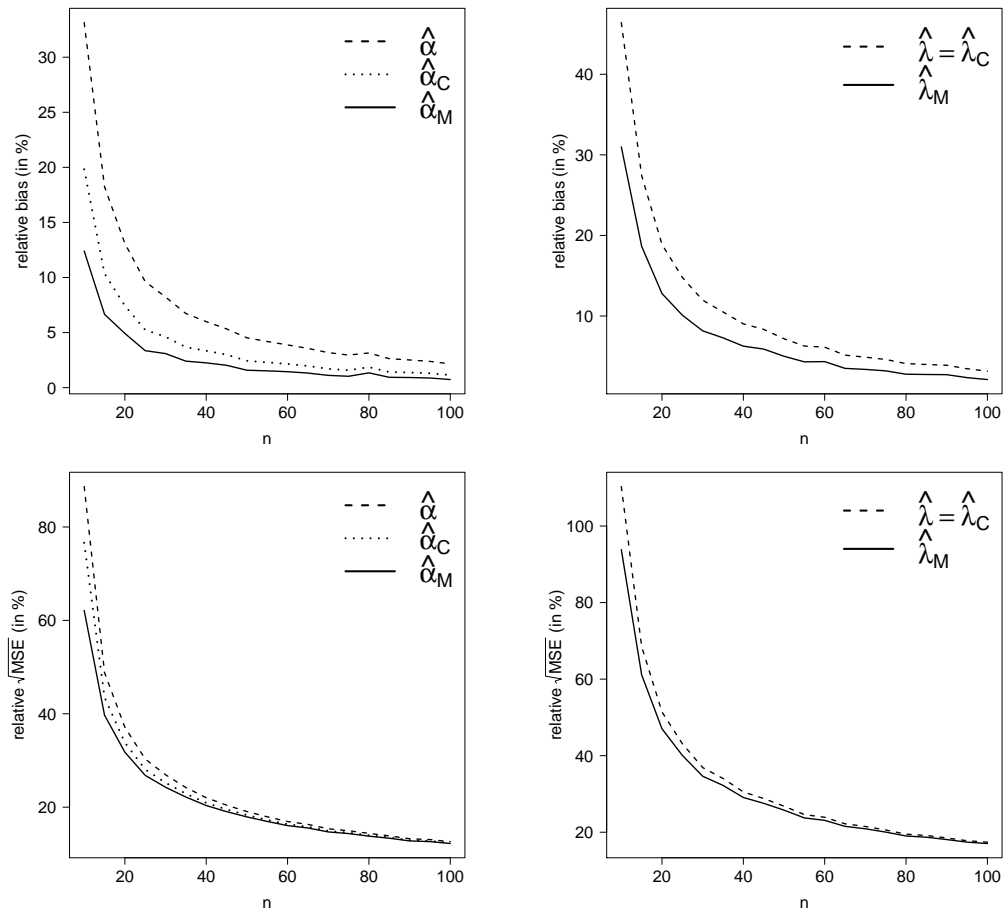


Figure 4: Estimated bias and root MSE for the MLEs and the modified MLEs in the $EE(\alpha = 0.5, \lambda = 0.05)$ model under different scenarios based on 10,000 replicates.

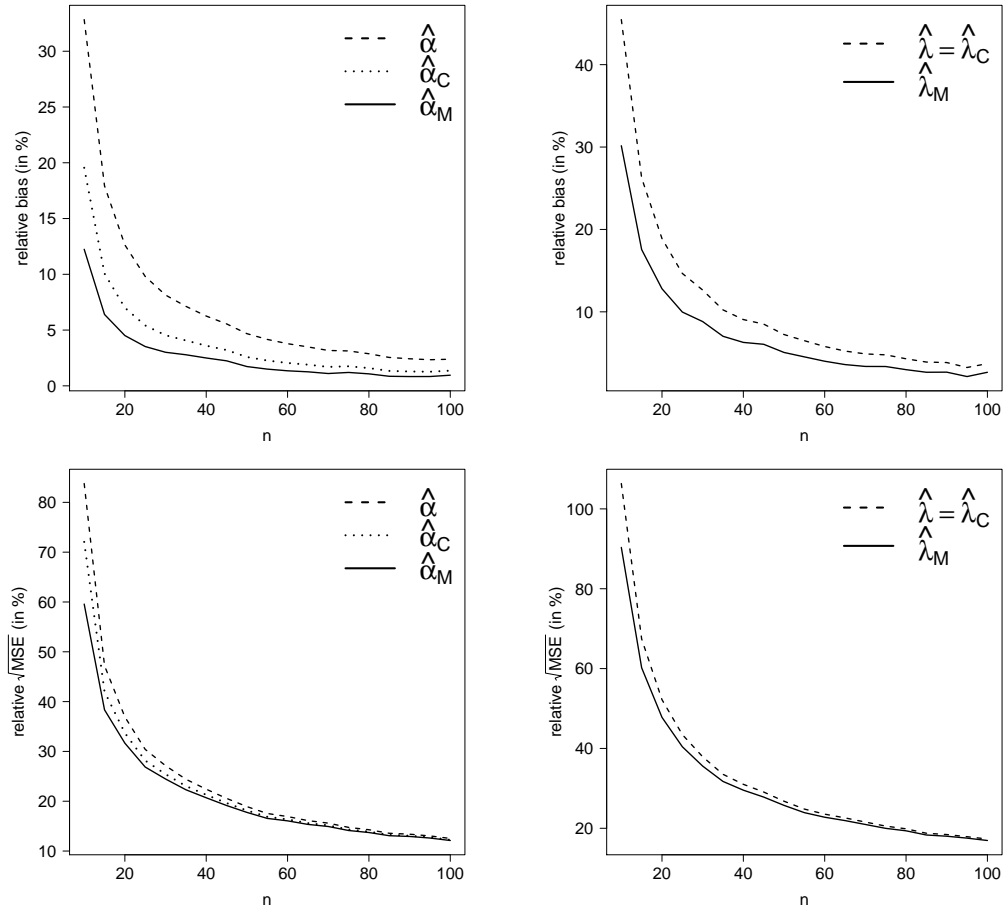


Figure 5: Estimated bias and root MSE for the MLEs and the modified MLEs in the $EE(\alpha = 0.5, \lambda = 0.1)$ model under different scenarios based on 10,000 replicates.

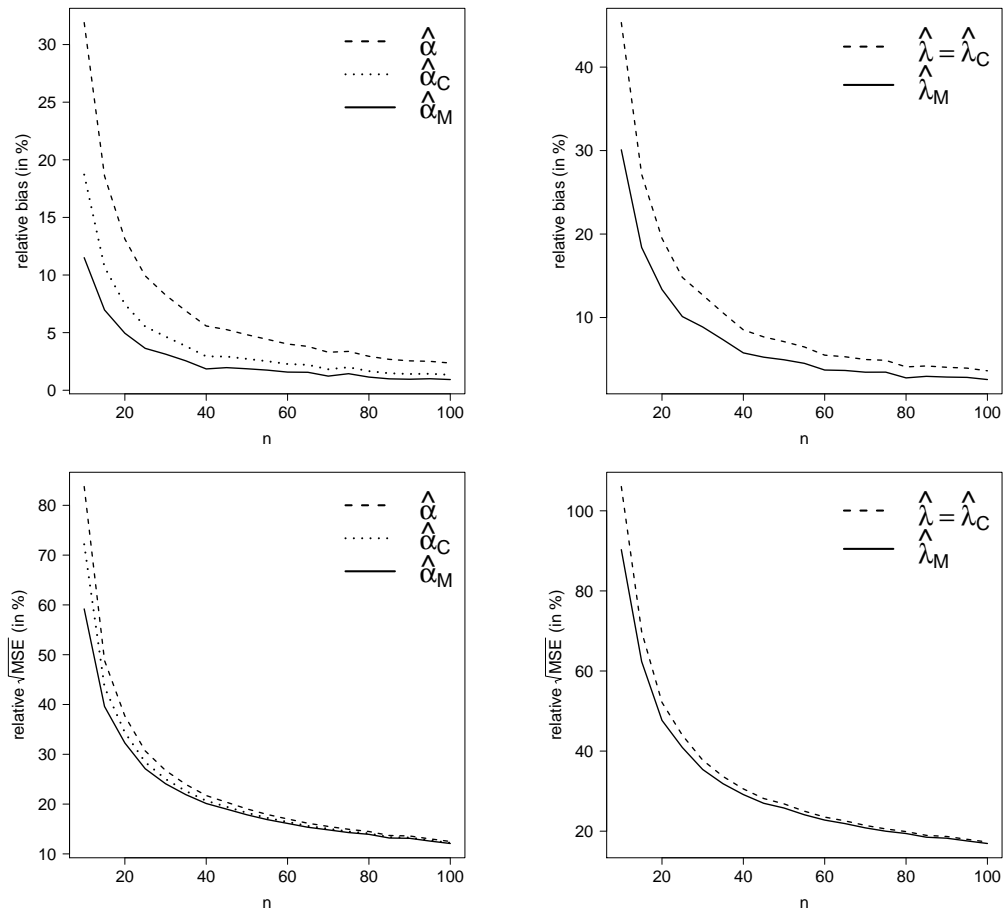


Figure 6: Estimated bias and root MSE for the MLEs and the modified MLEs in the $EE(\alpha = 0.5, \lambda = 0.2)$ model under different scenarios based on 10,000 replicates.

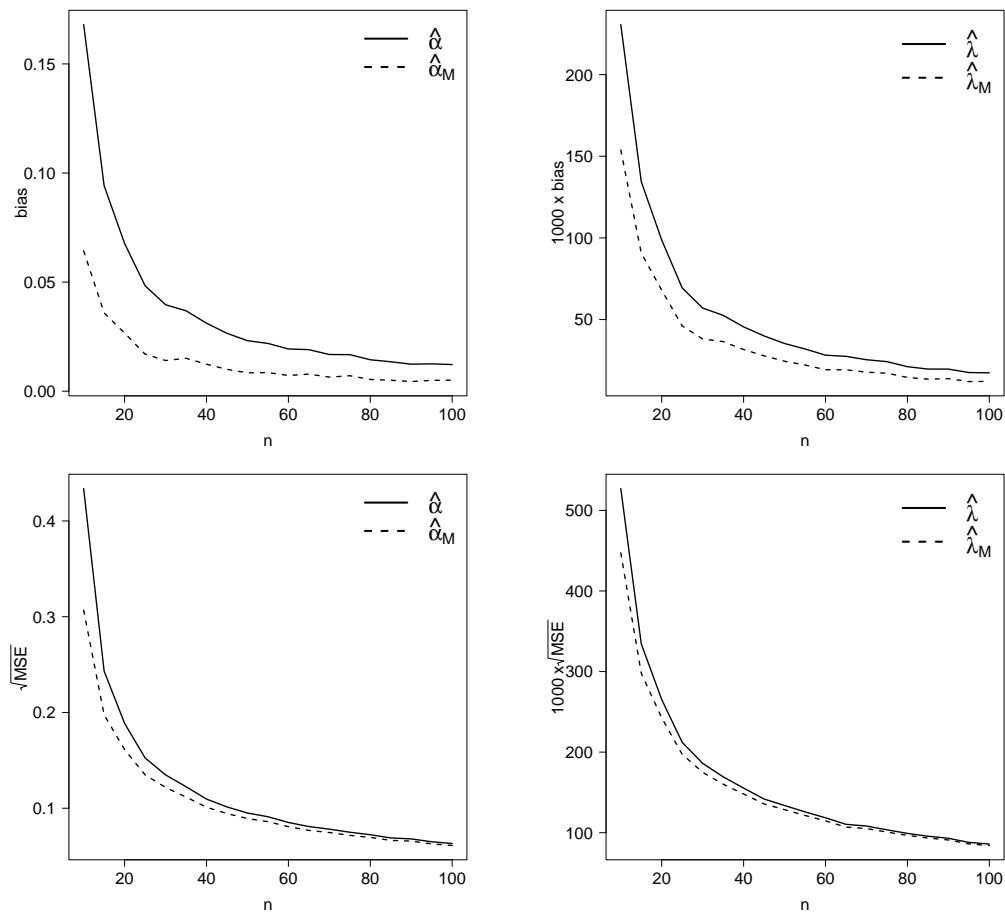


Figure 7: Estimated bias and root MSE for the MLEs and the modified MLEs in the $EE(\alpha = 0.5, \lambda = 0.5)$ model under different scenarios based on 10,000 replicates.

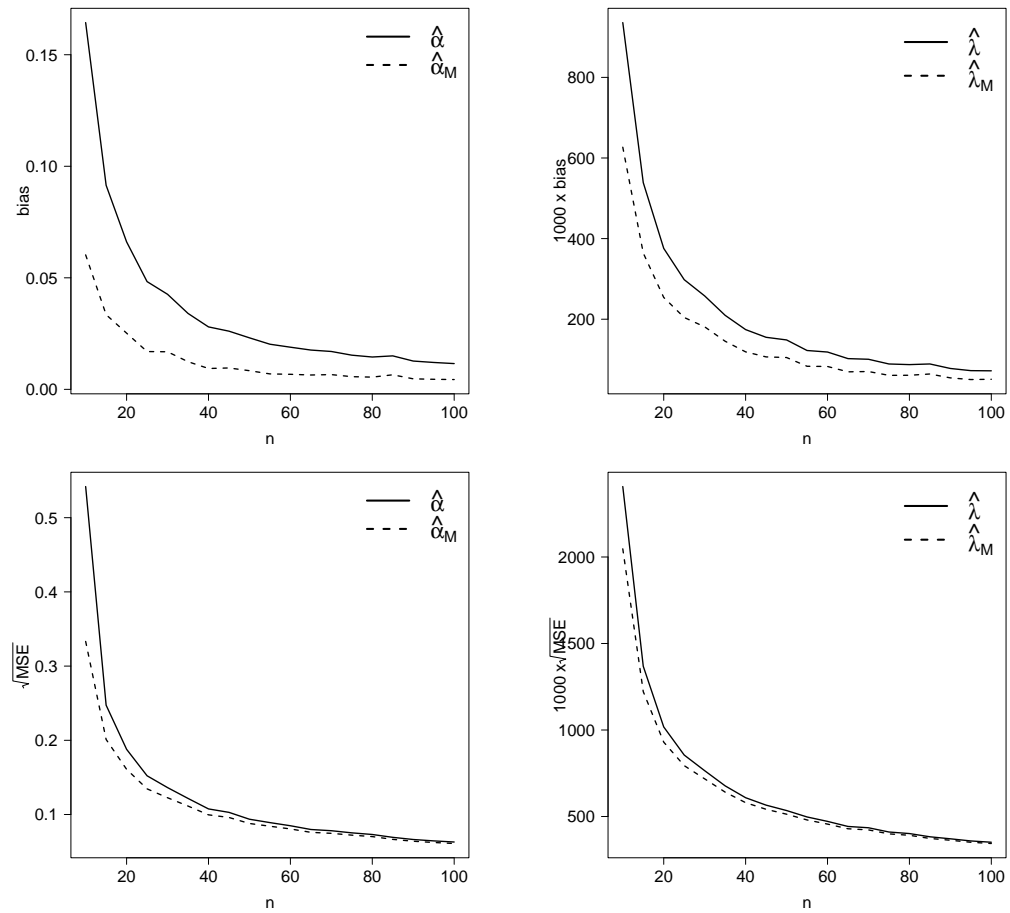


Figure 8: Estimated bias and root MSE for the MLEs and the modified MLEs in the EE($\alpha = 0.5, \lambda = 2$) model under different scenarios based on 10,000 replicates.

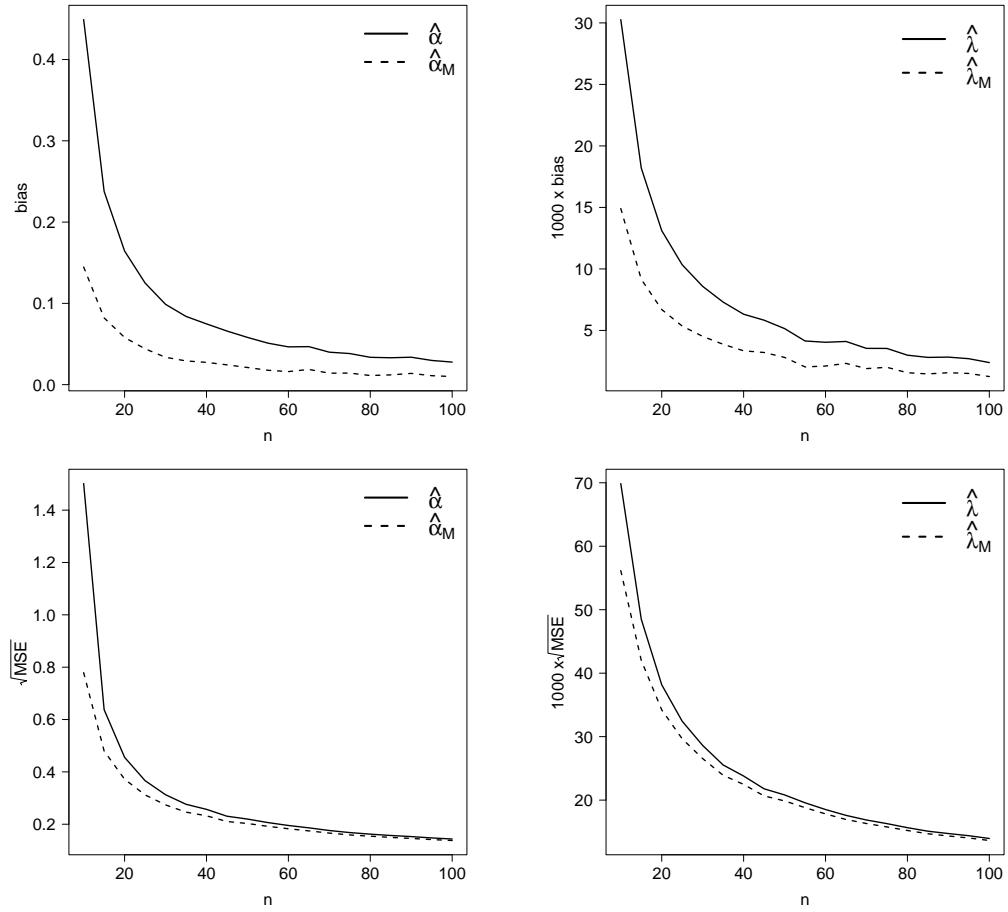


Figure 9: Estimated bias and root MSE for the MLEs and the modified MLEs in the EE($\alpha = 1, \lambda = 0.1$) model under different scenarios based on 10,000 replicates.

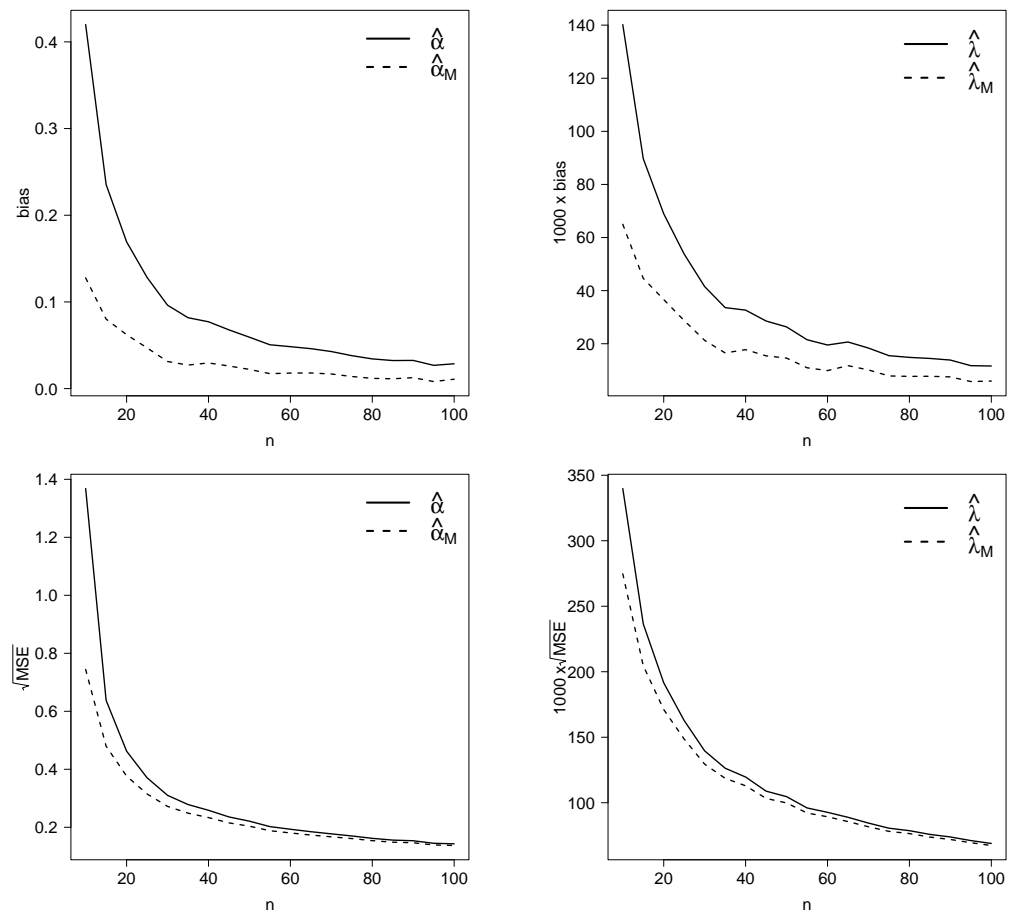


Figure 10: Estimated bias and root MSE for the MLEs and the modified MLEs in the EE($\alpha = 1, \lambda = 0.5$) model under different scenarios based on 10,000 replicates.

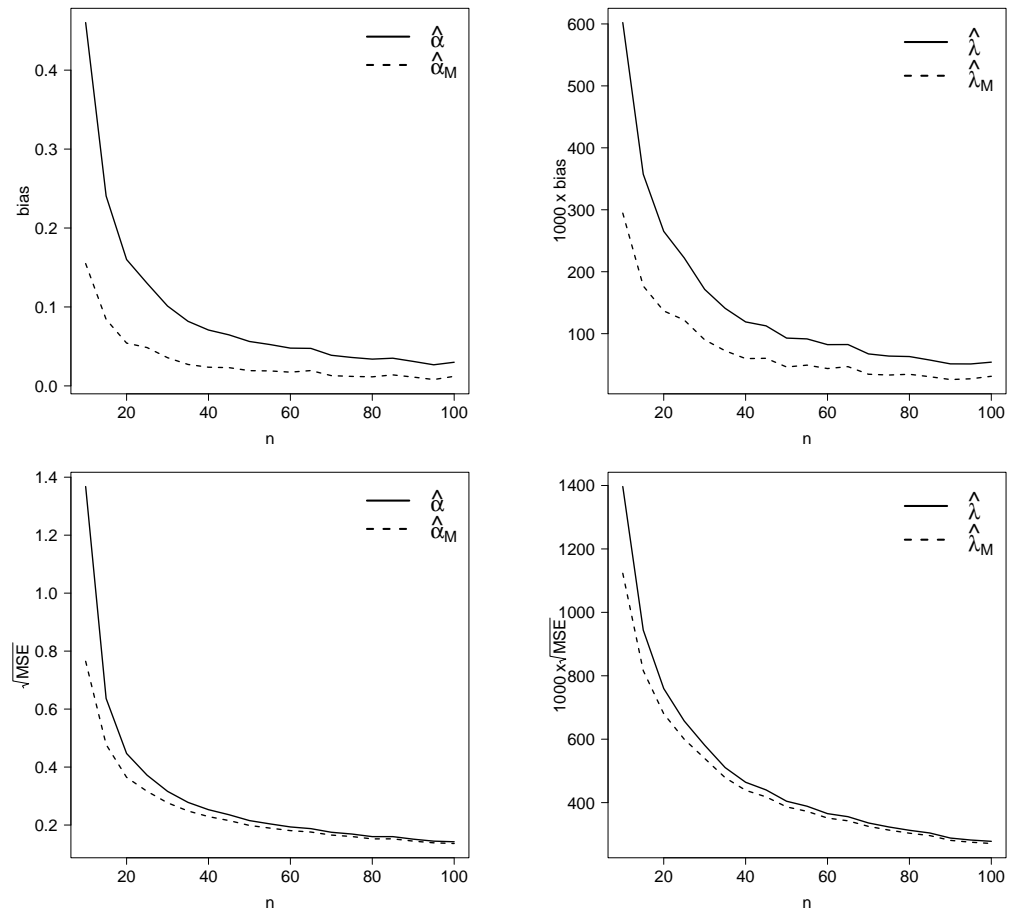


Figure 11: Estimated bias and root MSE for the MLEs and the modified MLEs in the EE($\alpha = 1, \lambda = 2$) model under different scenarios based on 10,000 replicates.

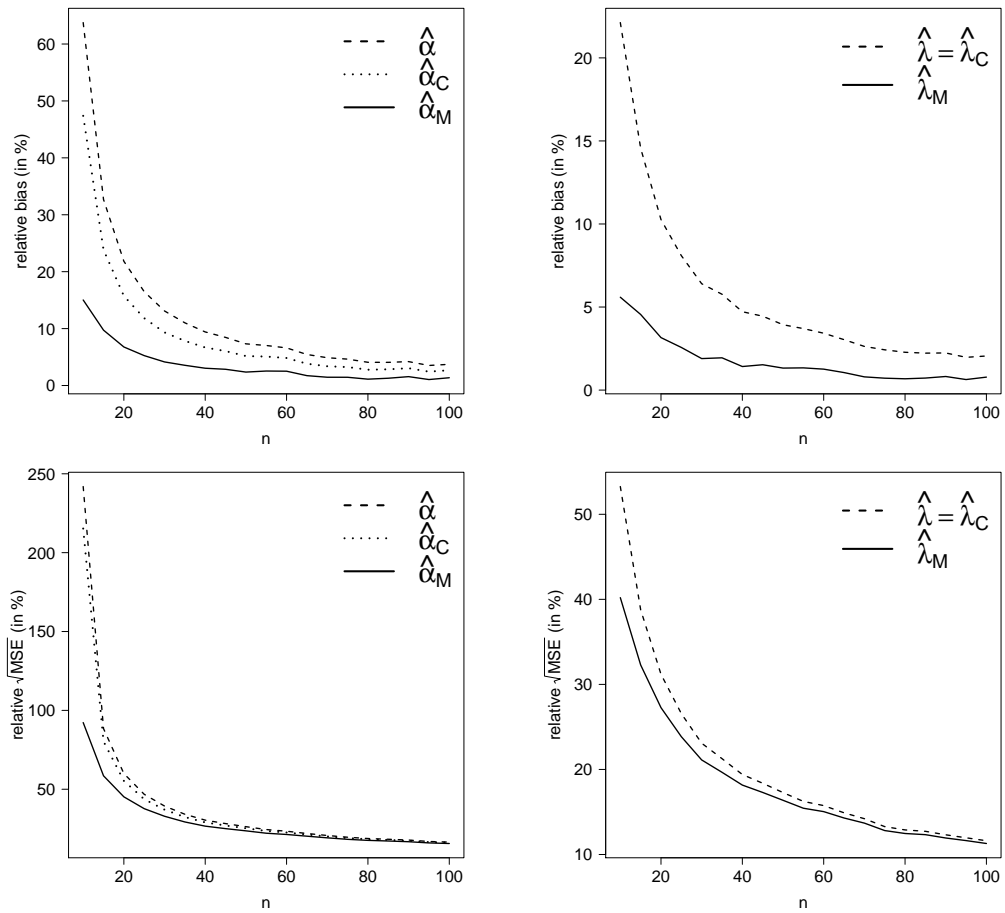


Figure 12: Estimated bias and root MSE for the MLEs and the modified MLEs in the $EE(\alpha = 2, \lambda = 0.05)$ model under different scenarios based on 10,000 replicates.

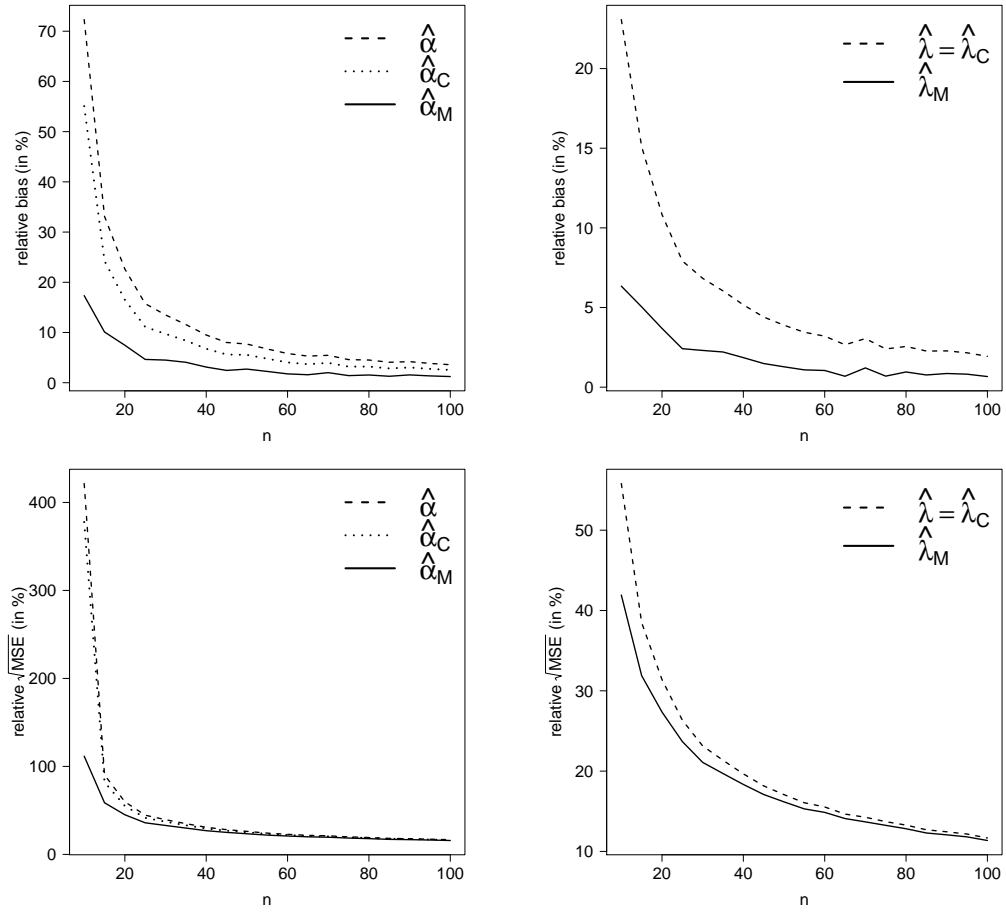


Figure 13: Estimated bias and root MSE for the MLEs and the modified MLEs in the EE($\alpha = 2, \lambda = 0.1$) model under different scenarios based on 10,000 replicates.

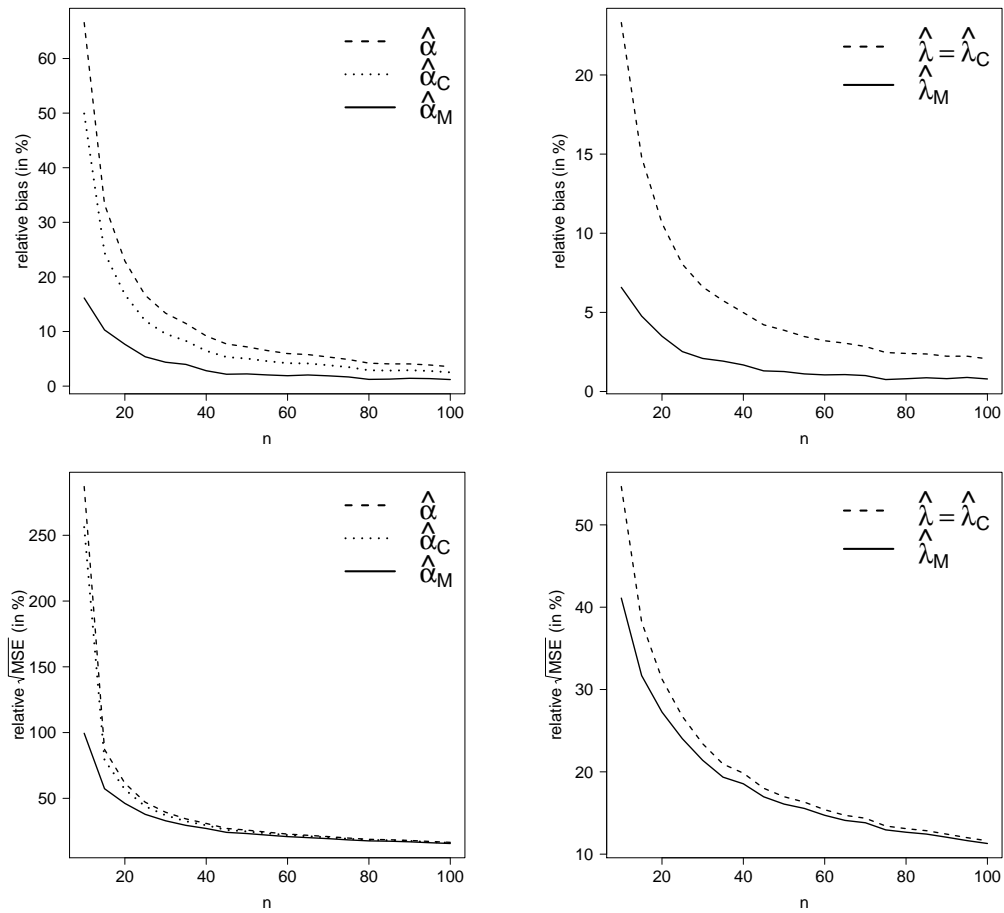


Figure 14: Estimated bias and root MSE for the MLEs and the modified MLEs in the $EE(\alpha = 2, \lambda = 0.2)$ model under different scenarios based on 10,000 replicates.

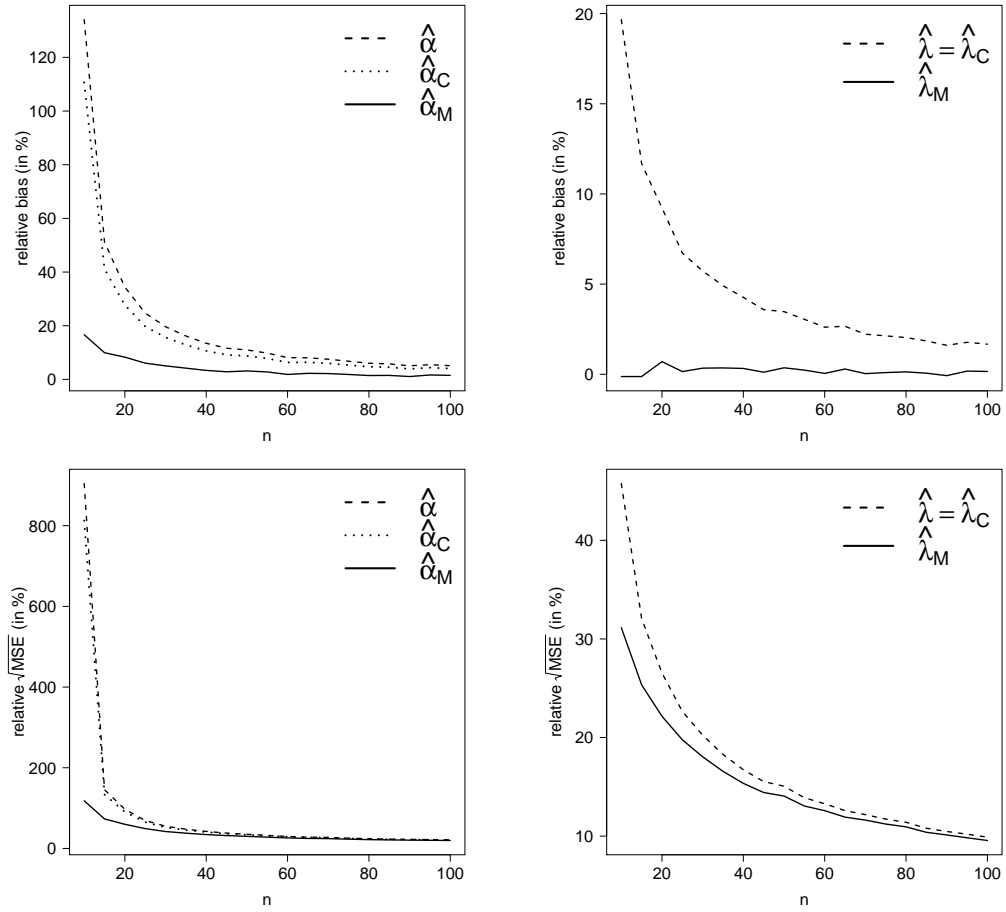


Figure 15: Estimated bias and root MSE for the MLEs and the modified MLEs in the $EE(\alpha = 5, \lambda = 0.05)$ model under different scenarios based on 10,000 replicates.

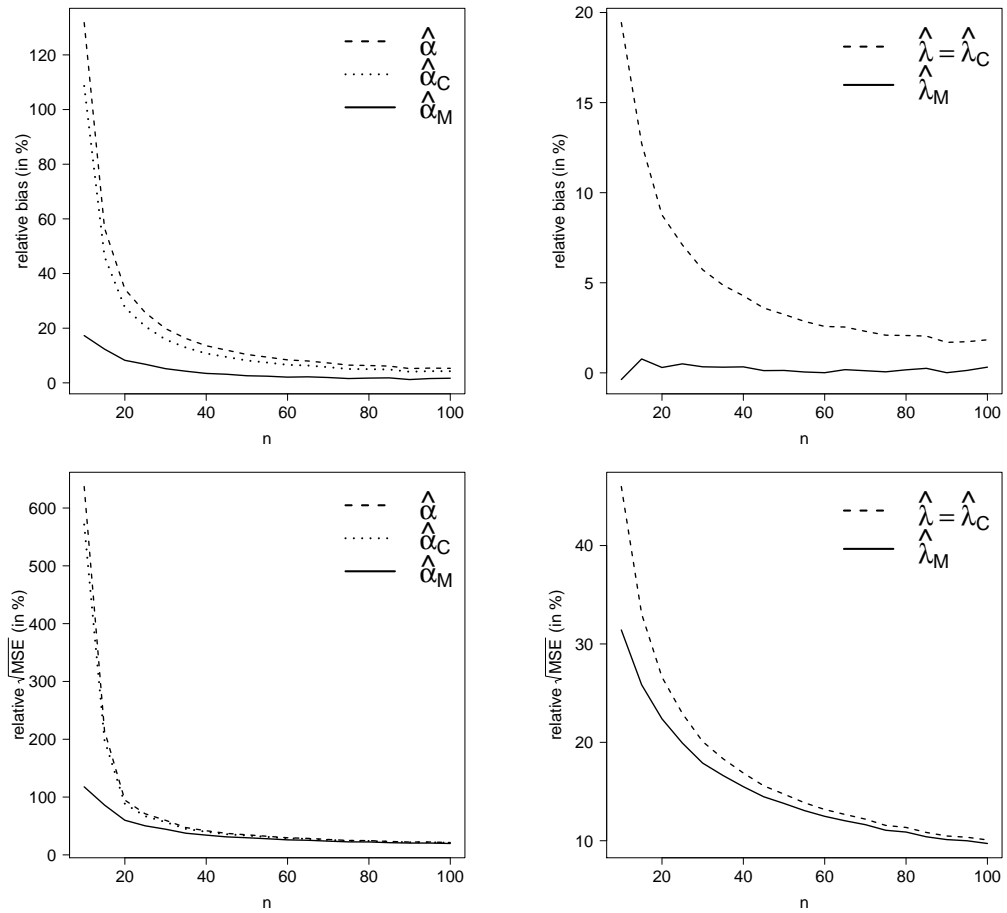


Figure 16: Estimated bias and root MSE for the MLEs and the modified MLEs in the $EE(\alpha = 5, \lambda = 0.1)$ model under different scenarios based on 10,000 replicates.

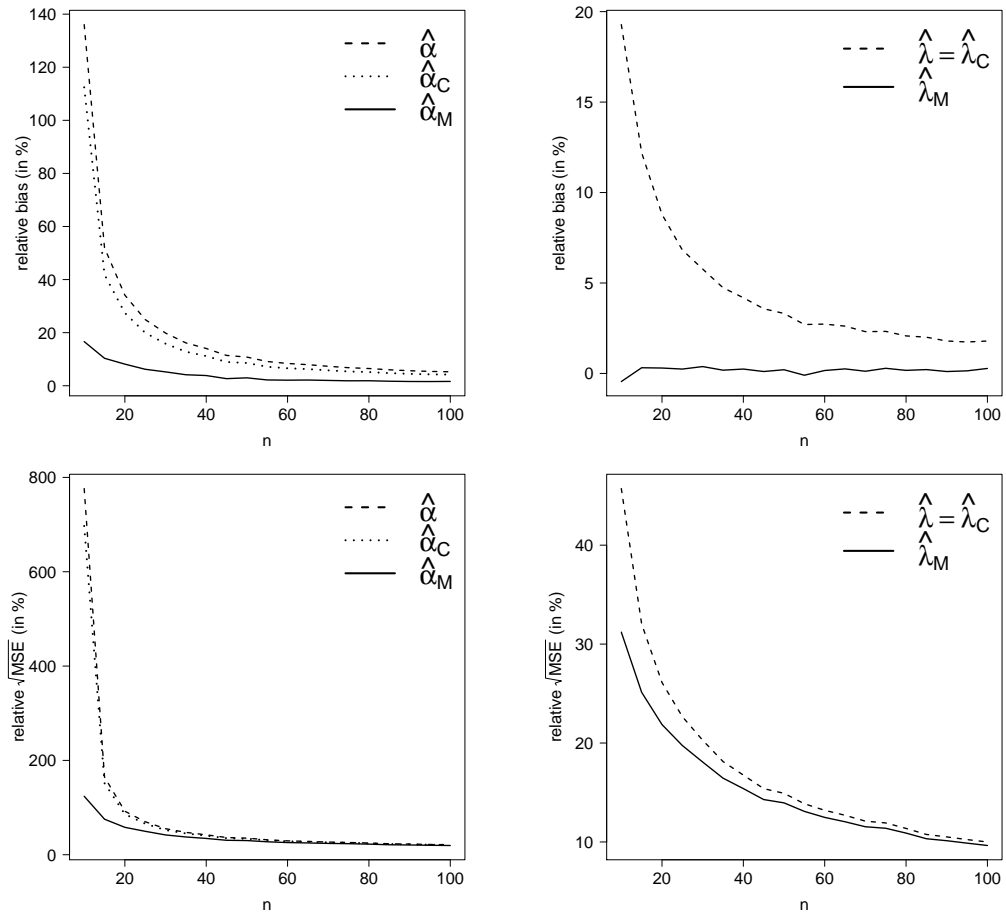


Figure 17: Estimated bias and root MSE for the MLEs and the modified MLEs in the $EE(\alpha = 5, \lambda = 0.2)$ model under different scenarios based on 10,000 replicates.

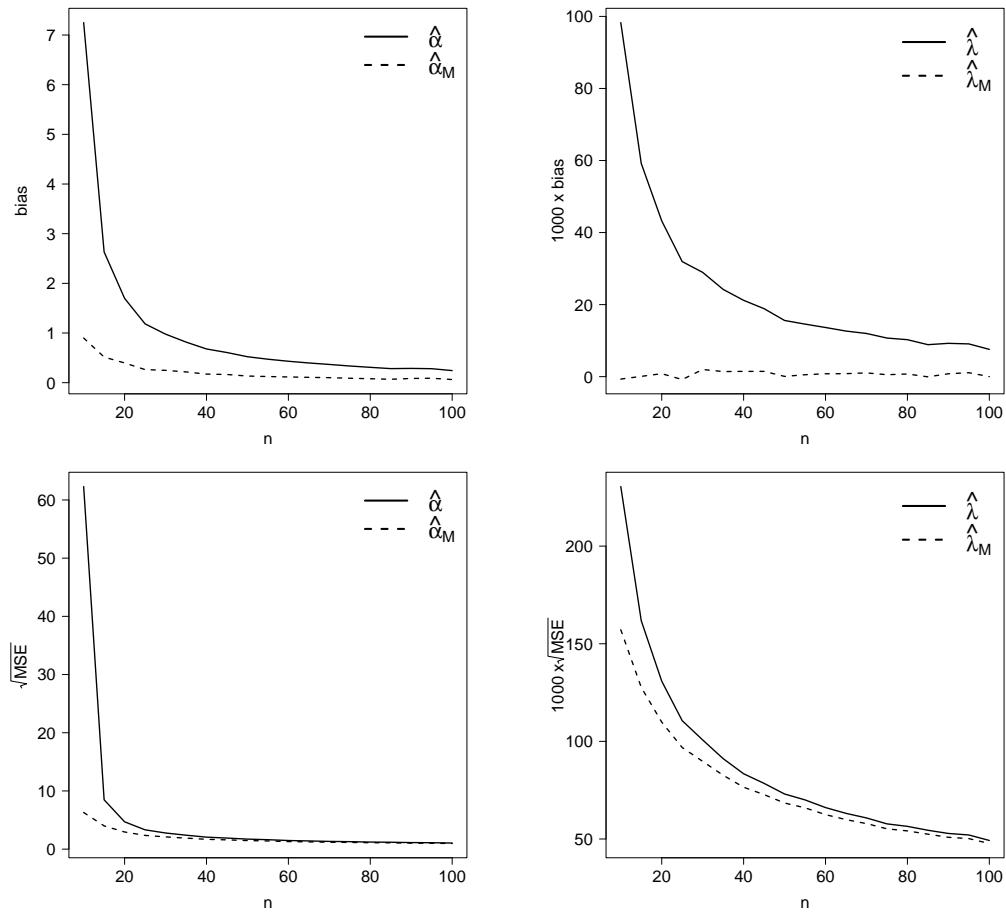


Figure 18: Estimated bias and root MSE for the MLEs and the modified MLEs in the $EE(\alpha = 5, \lambda = 0.5)$ model under different scenarios based on 10,000 replicates.

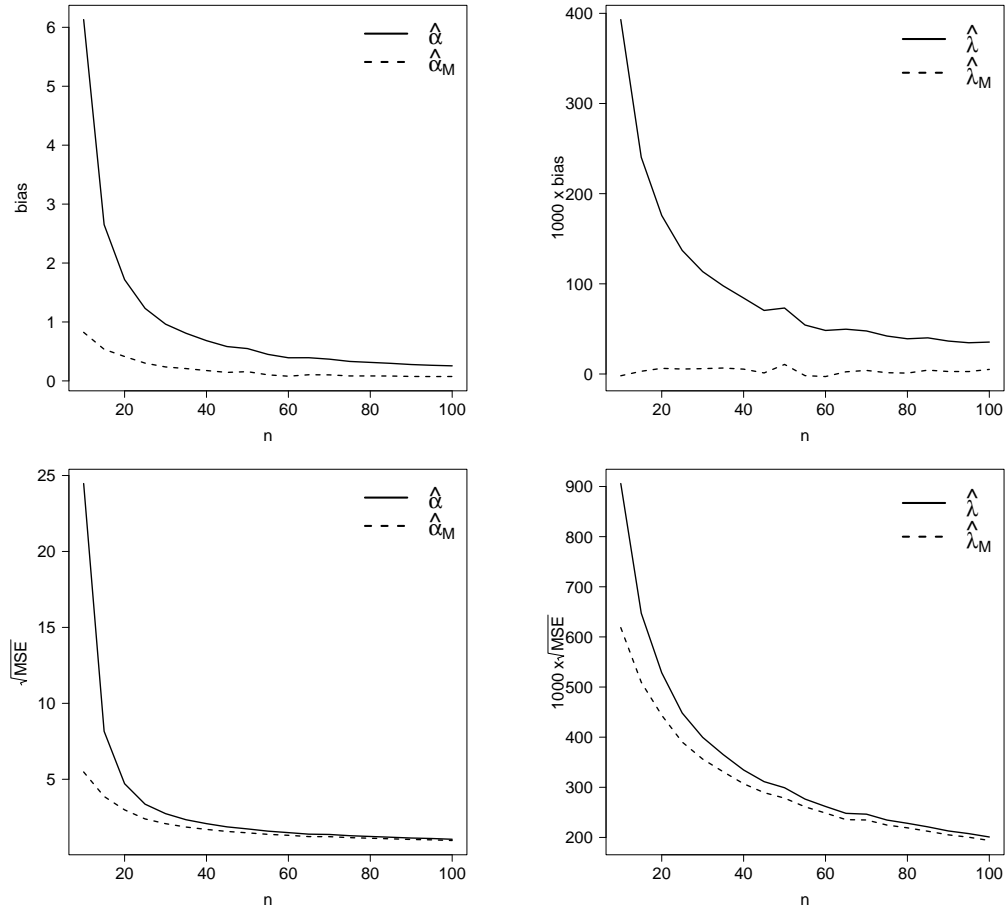


Figure 19: Estimated bias and root MSE for the MLEs and the modified MLEs in the EE($\alpha = 5, \lambda = 2$) model under different scenarios based on 10,000 replicates.

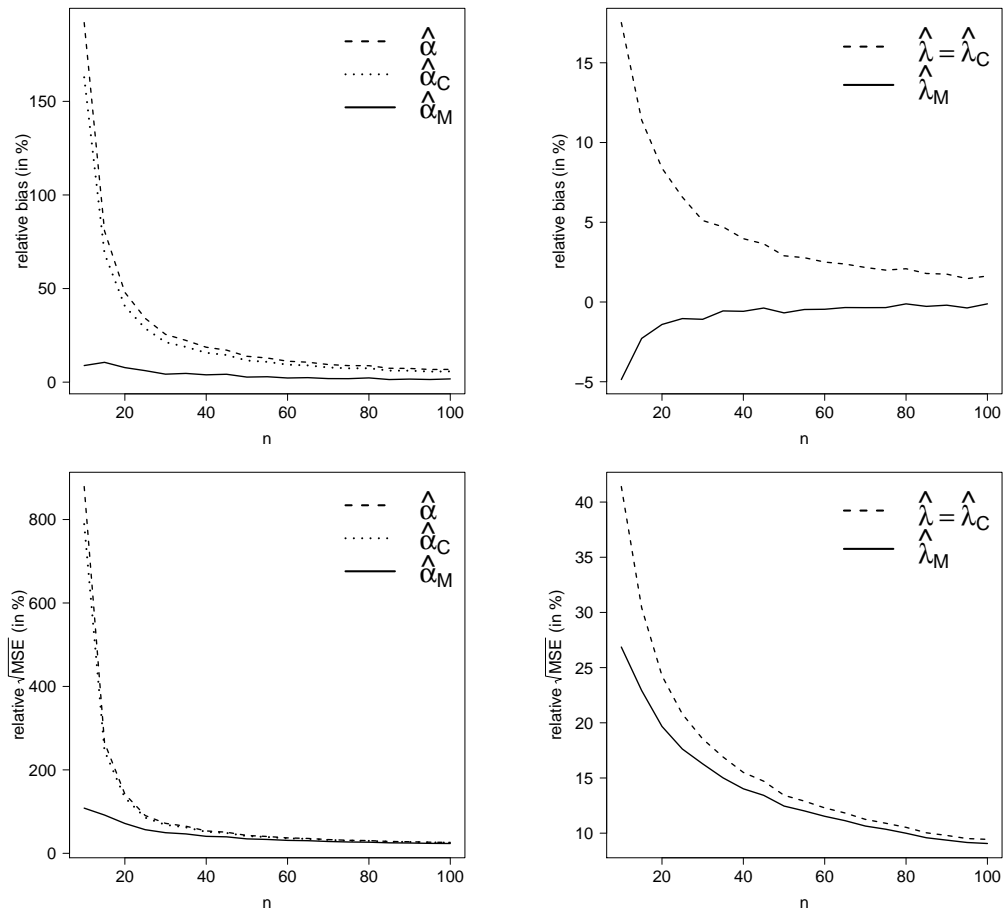


Figure 20: Estimated bias and root MSE for the MLEs and the modified MLEs in the EE($\alpha = 10, \lambda = 0.05$) model under different scenarios based on 10,000 replicates.

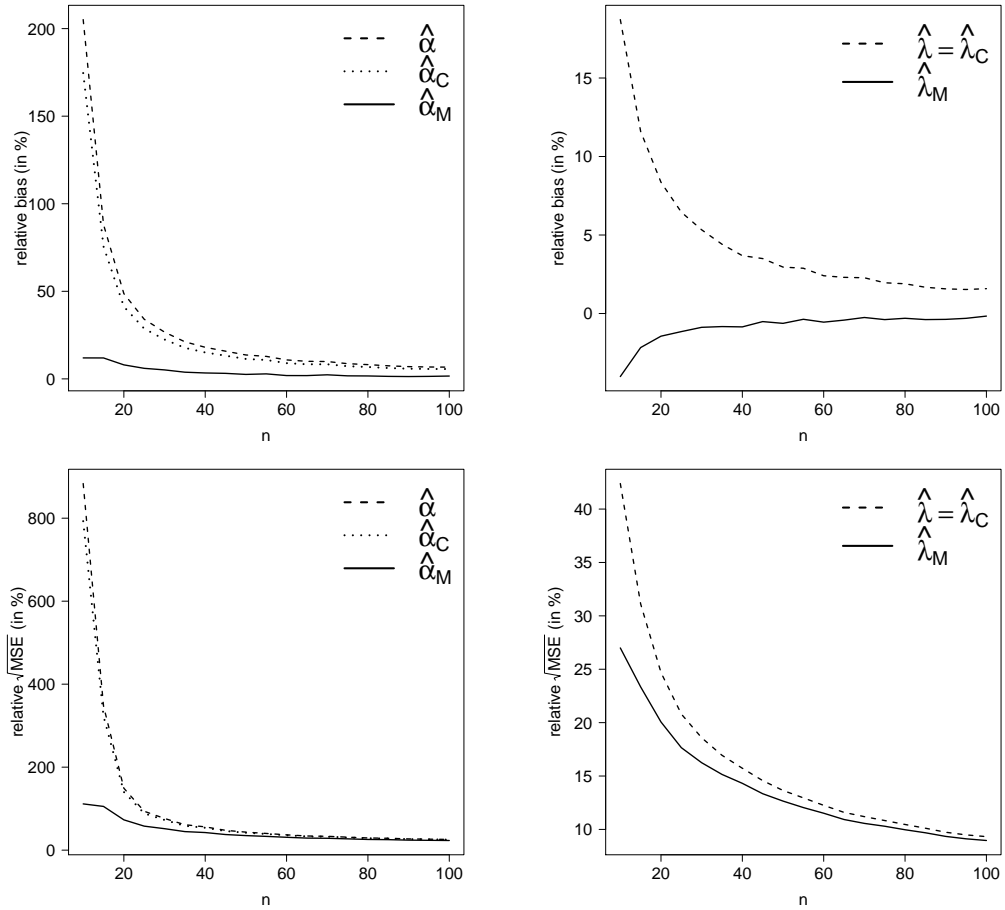


Figure 21: Estimated bias and root MSE for the MLEs and the modified MLEs in the EE($\alpha = 10, \lambda = 0.1$) model under different scenarios based on 10,000 replicates.

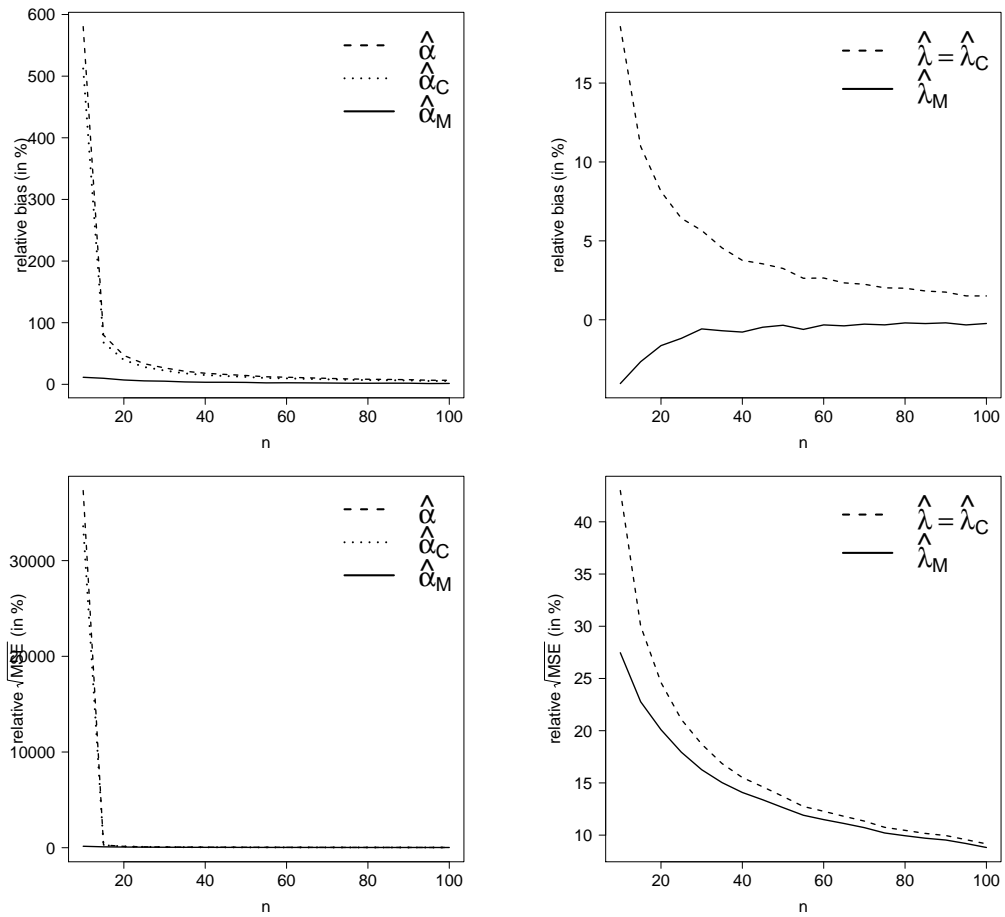


Figure 22: Estimated bias and root MSE for the MLEs and the modified MLEs in the EE($\alpha = 10, \lambda = 0.2$) model under different scenarios based on 10,000 replicates.

1.2. PHN distribution

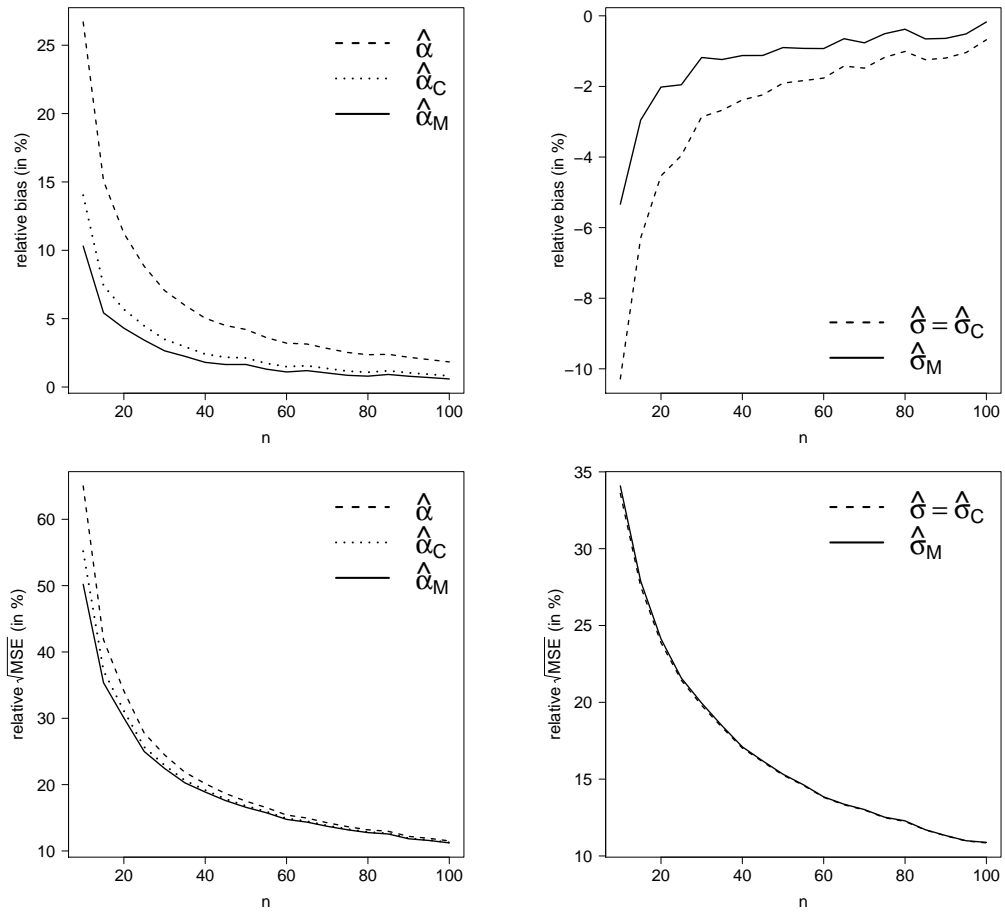


Figure 23: Estimated bias and root MSE for the MLEs and the modified MLEs in the PHN($\alpha = 0.5, \sigma = 5$) model under different scenarios based on 10,000 replicates.

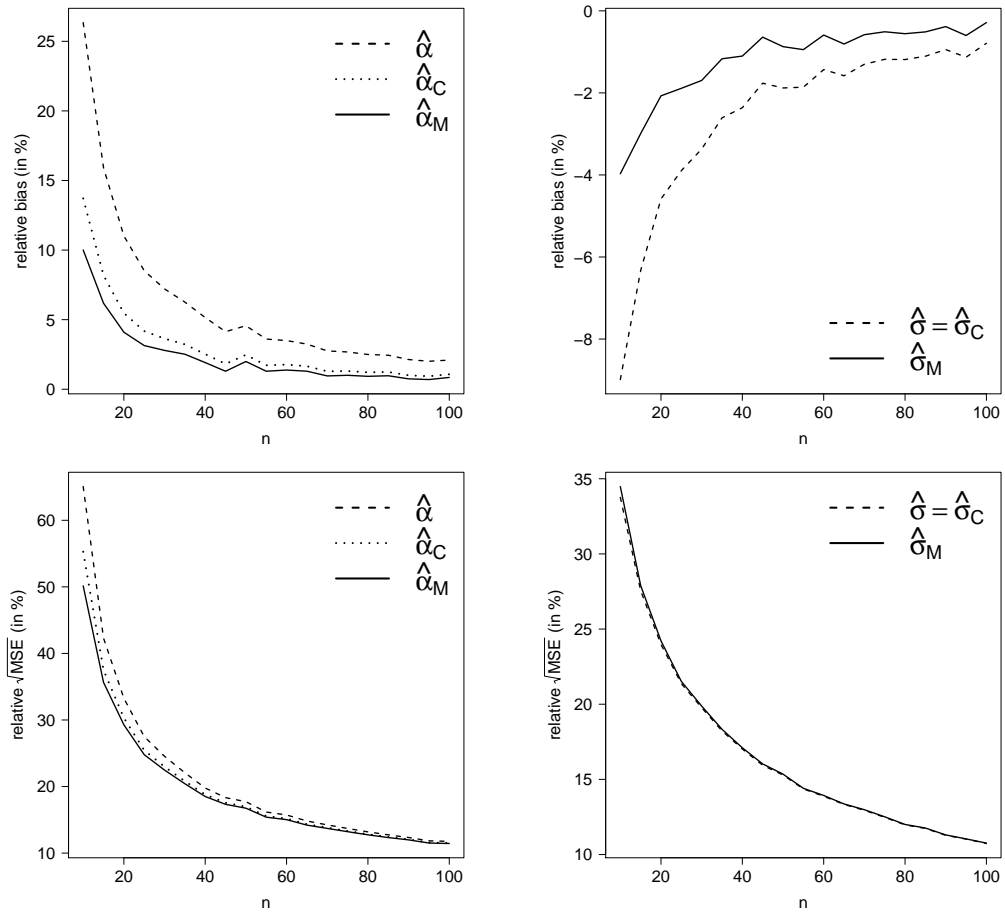


Figure 24: Estimated bias and root MSE for the MLEs and the modified MLEs in the PHN($\alpha = 0.5, \sigma = 30$) model under different scenarios based on 10,000 replicates.

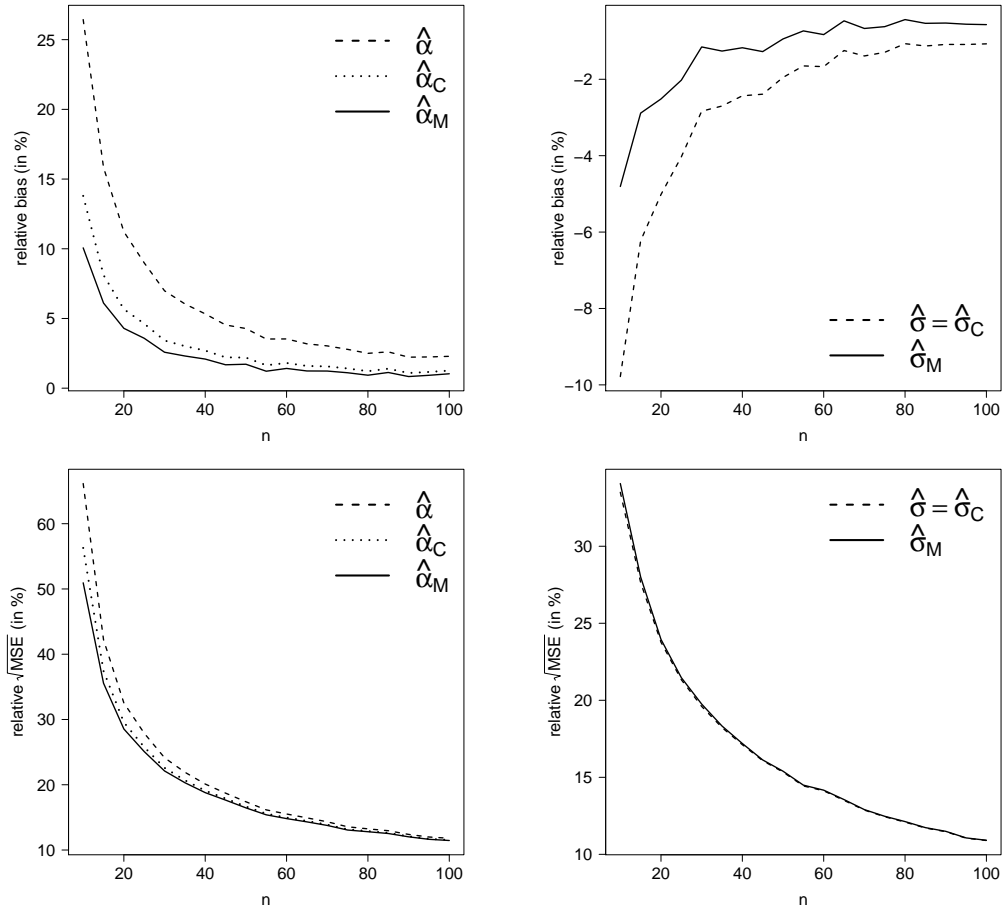


Figure 25: Estimated bias and root MSE for the MLEs and the modified MLEs in the PHN($\alpha = 0.5, \sigma = 50$) model under different scenarios based on 10,000 replicates.

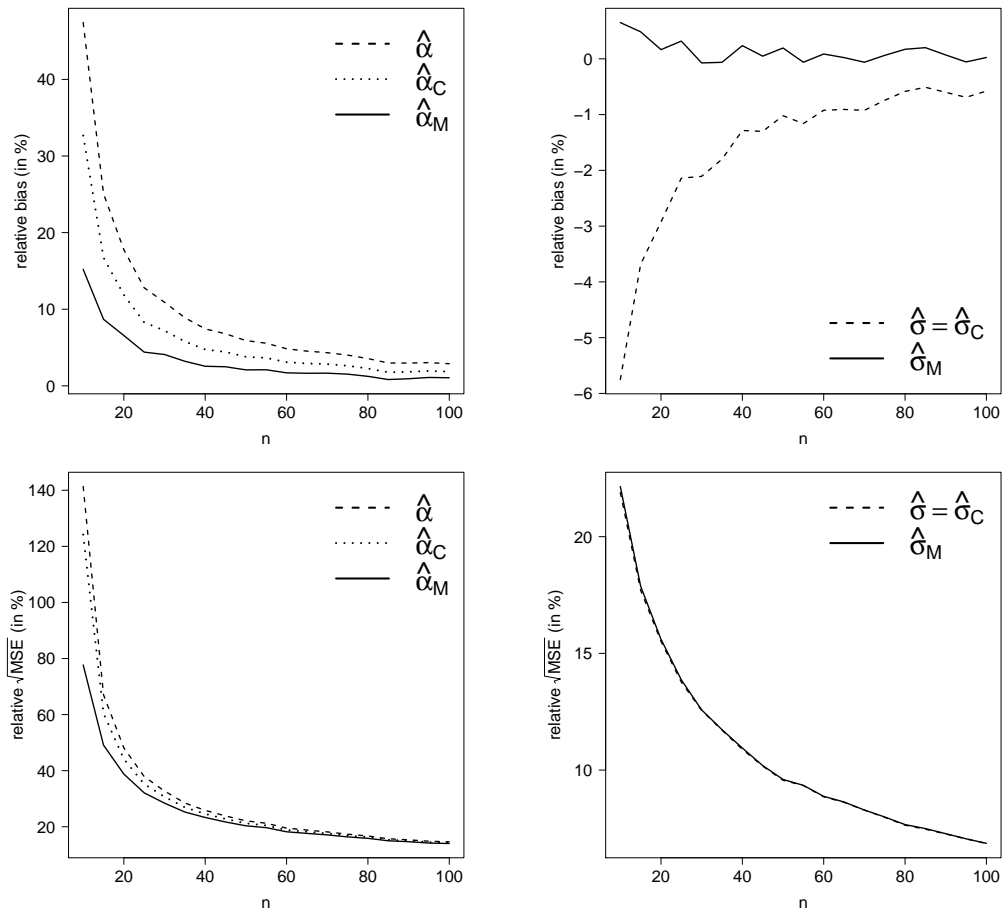


Figure 26: Estimated bias and root MSE for the MLEs and the modified MLEs in the PHN($\alpha = 2, \sigma = 5$) model under different scenarios based on 10,000 replicates.

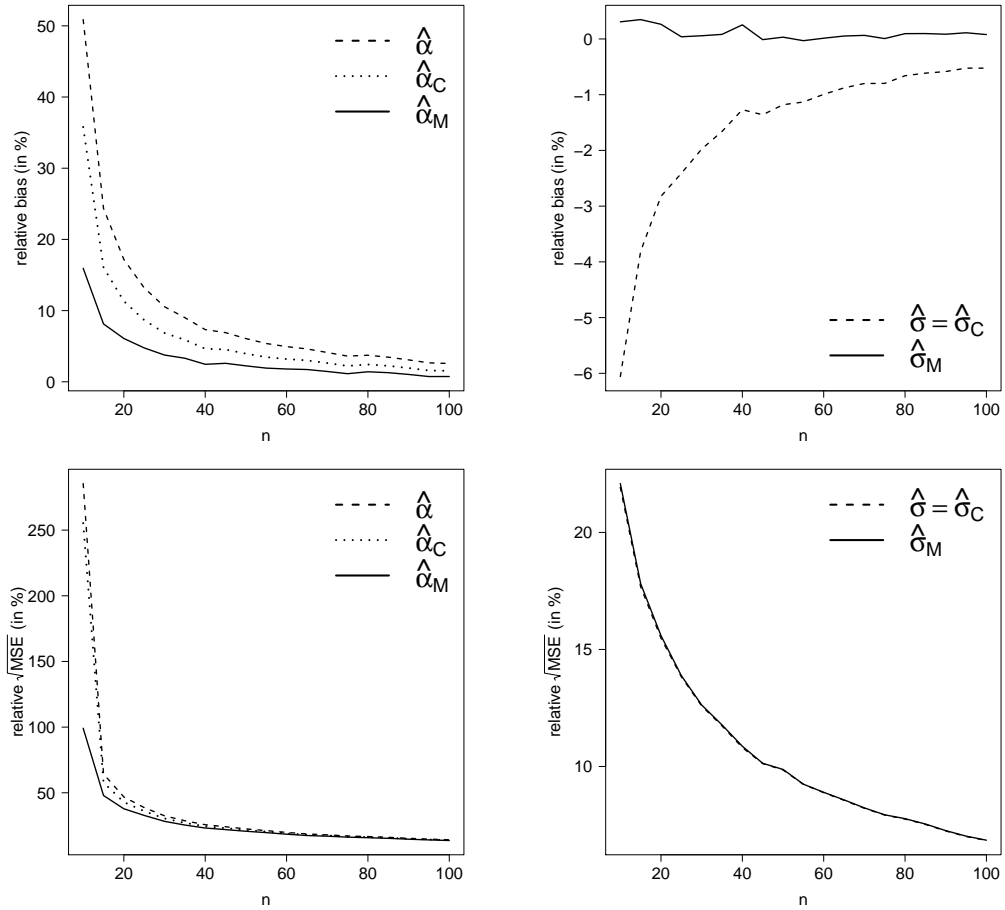


Figure 27: Estimated bias and root MSE for the MLEs and the modified MLEs in the PHN($\alpha = 2, \sigma = 30$) model under different scenarios based on 10,000 replicates.

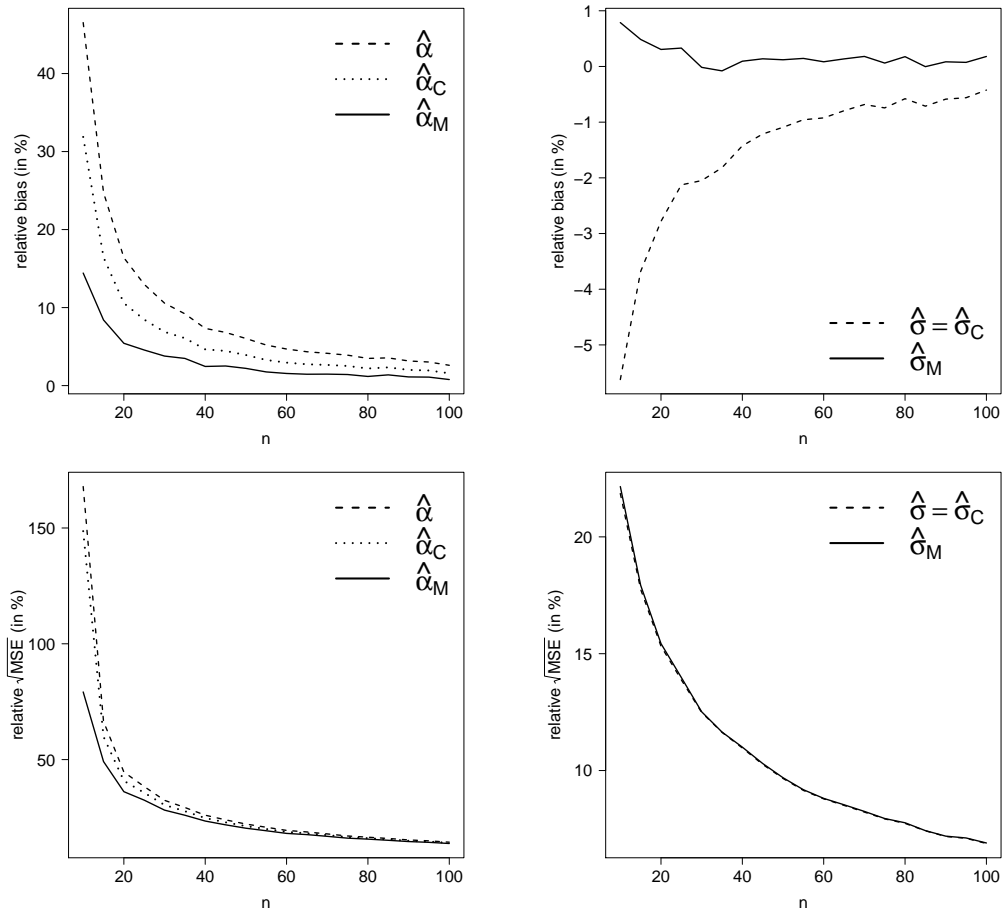


Figure 28: Estimated bias and root MSE for the MLEs and the modified MLEs in the PHN($\alpha = 2, \sigma = 50$) model under different scenarios based on 10,000 replicates.

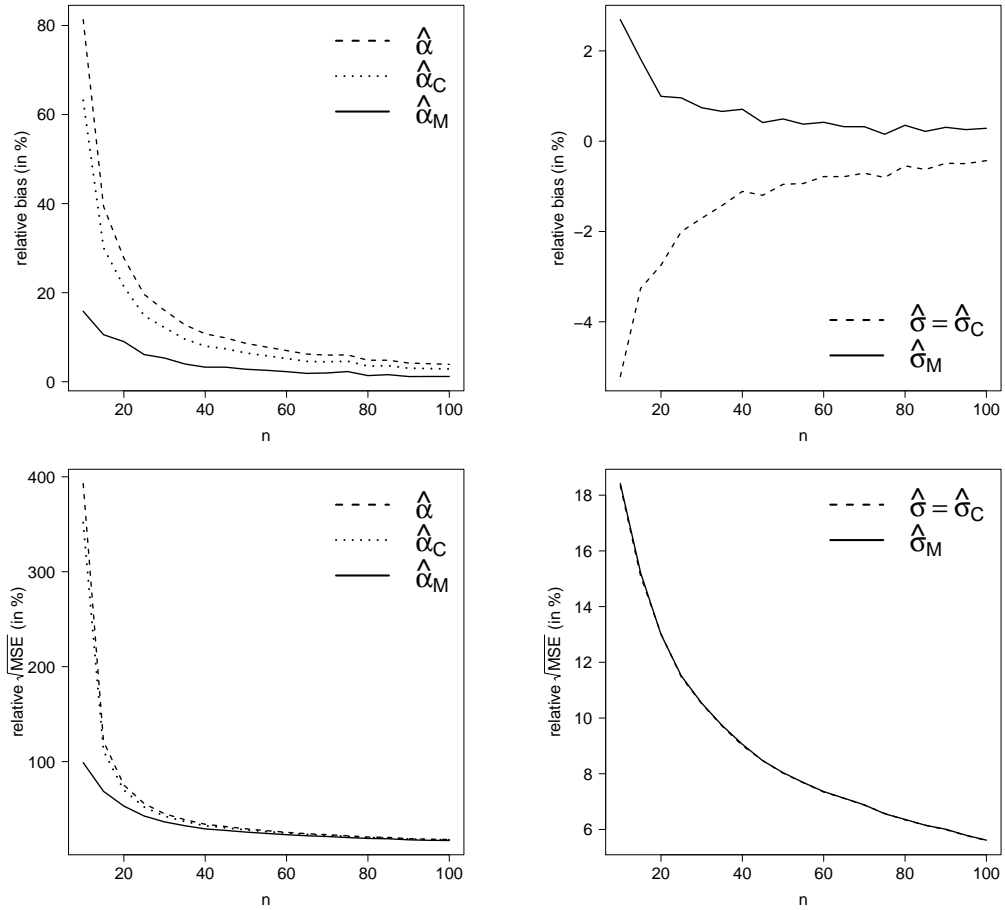


Figure 29: Estimated bias and root MSE for the MLEs and the modified MLEs in the PHN($\alpha = 5, \sigma = 5$) model under different scenarios based on 10,000 replicates.

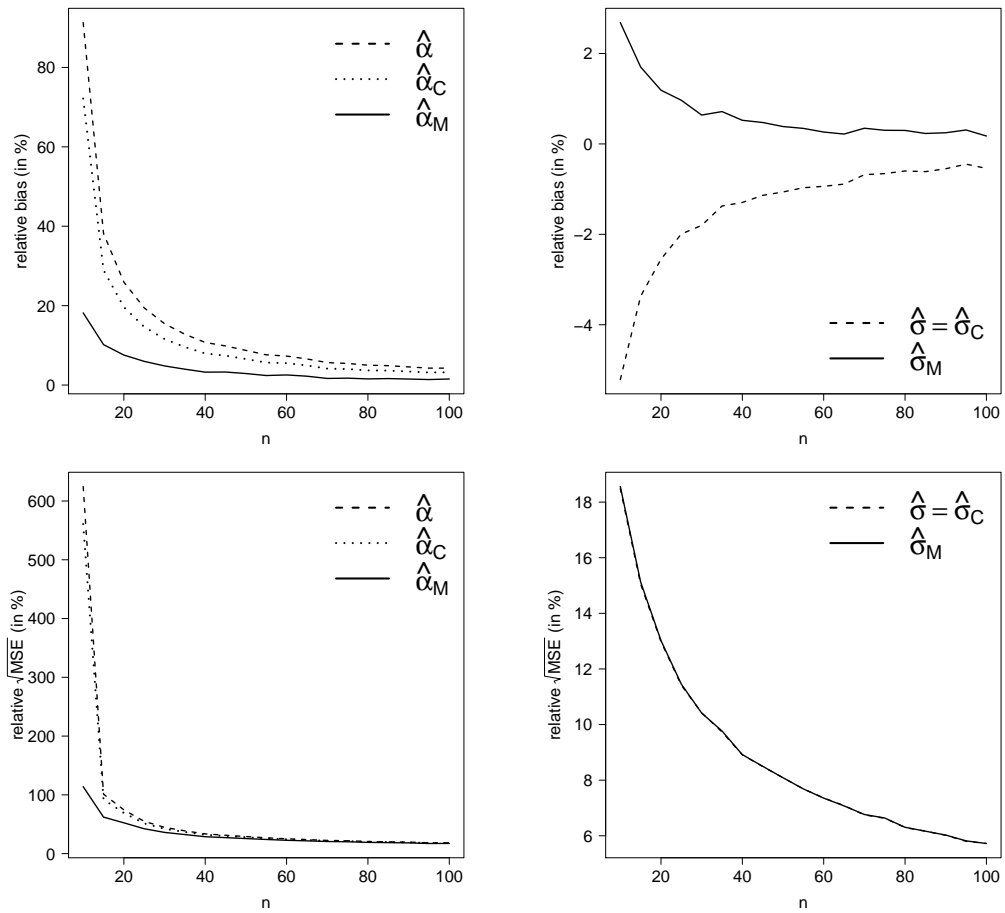


Figure 30: Estimated bias and root MSE for the MLEs and the modified MLEs in the PHN($\alpha = 5, \sigma = 30$) model under different scenarios based on 10,000 replicates.

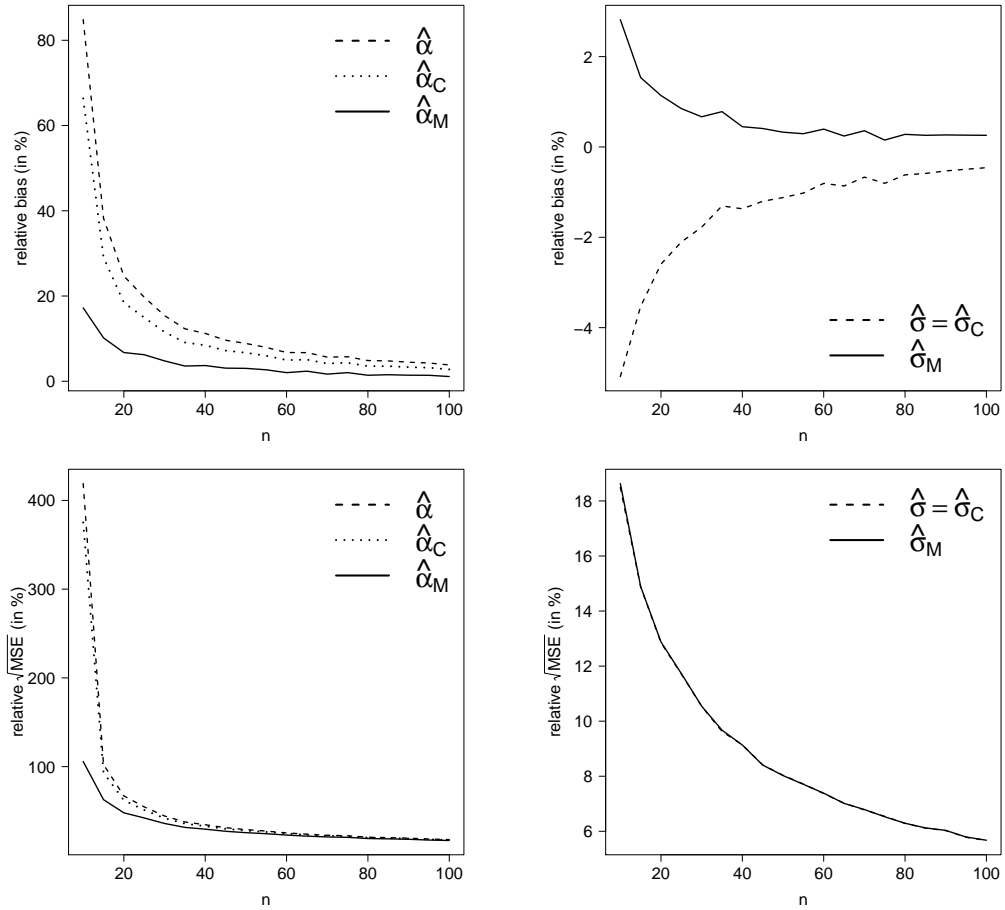


Figure 31: Estimated bias and root MSE for the MLEs and the modified MLEs in the PHN($\alpha = 5, \sigma = 50$) model under different scenarios based on 10,000 replicates.

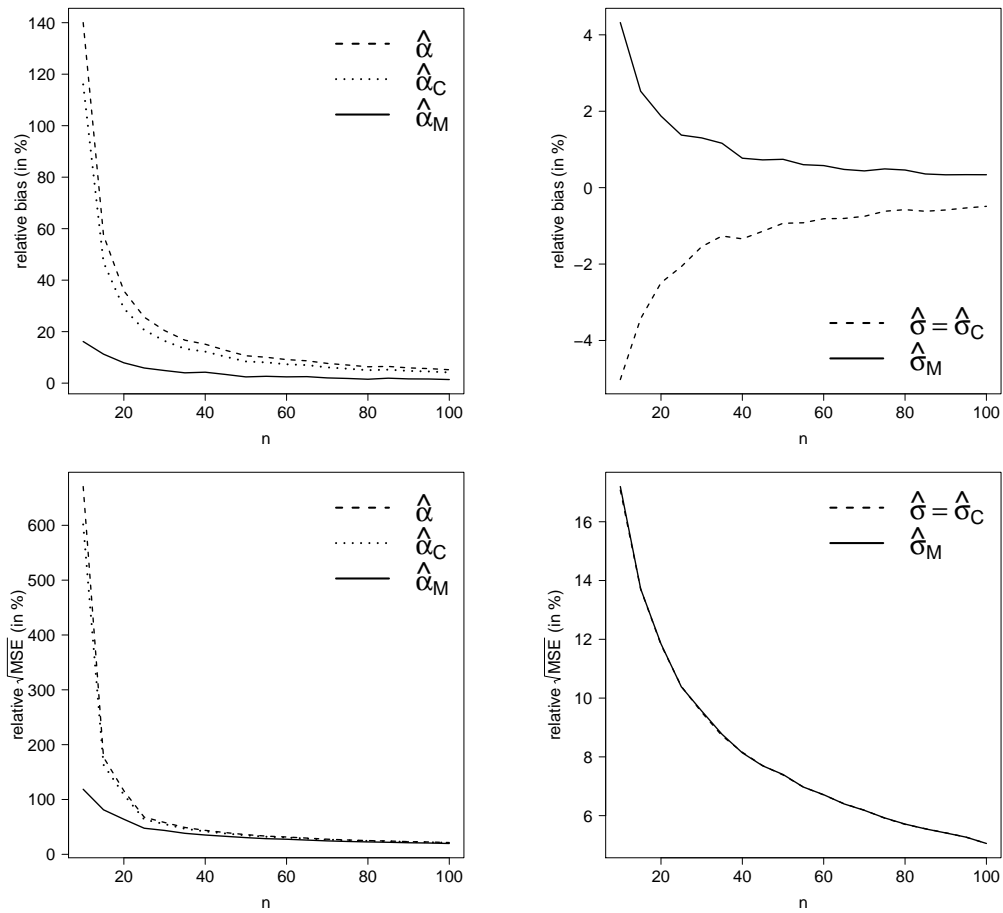


Figure 32: Estimated bias and root MSE for the MLEs and the modified MLEs in the PHN($\alpha = 10, \sigma = 5$) model under different scenarios based on 10,000 replicates.

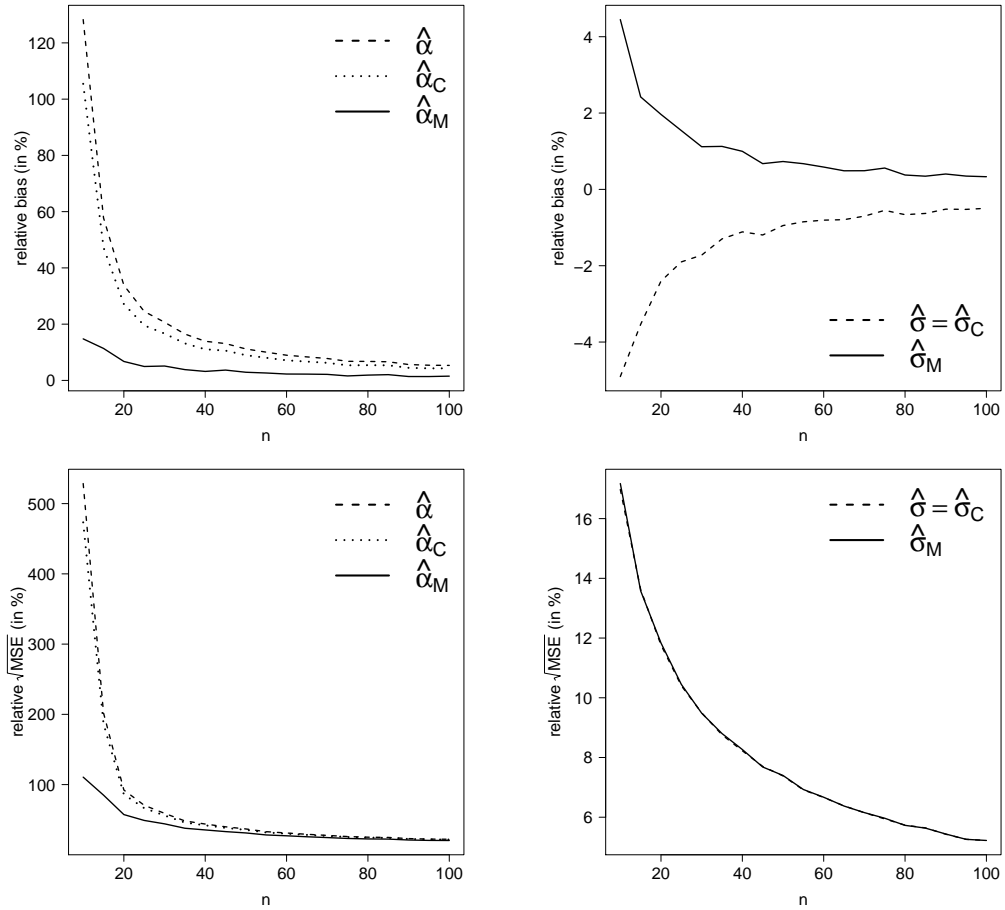


Figure 33: Estimated bias and root MSE for the MLEs and the modified MLEs in the PHN($\alpha = 10, \sigma = 30$) model under different scenarios based on 10,000 replicates.

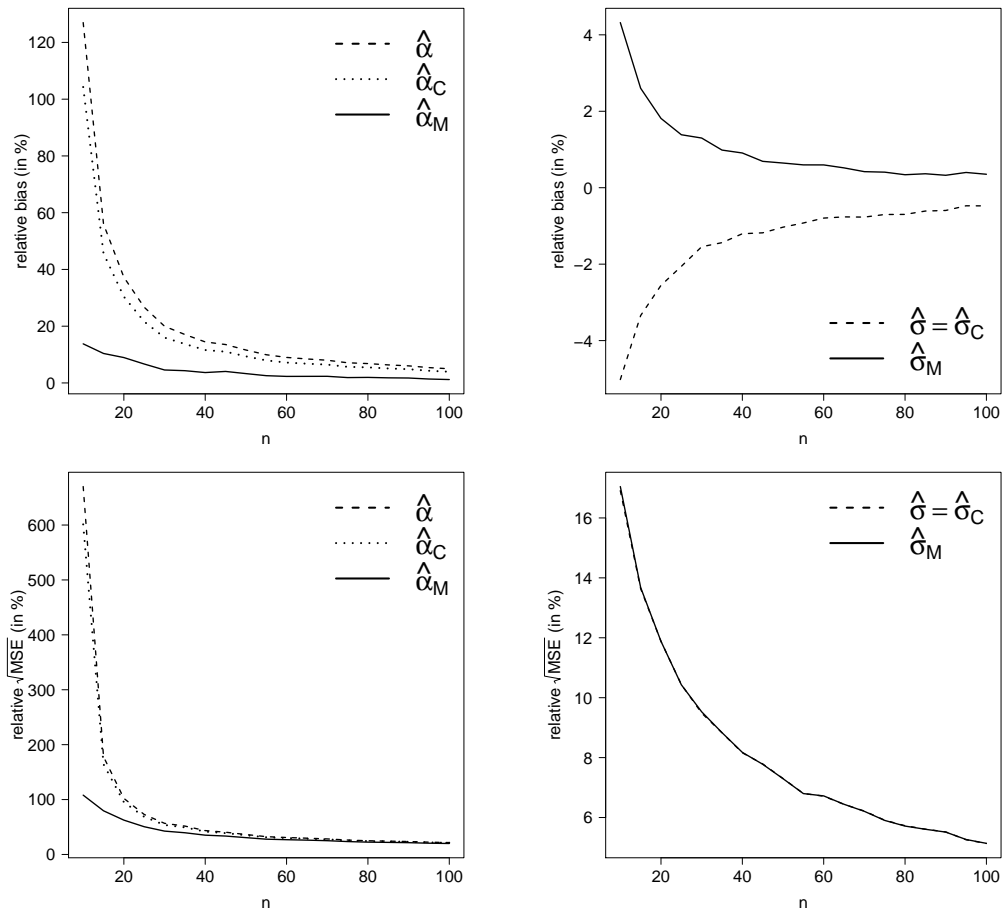


Figure 34: Estimated bias and root MSE for the MLEs and the modified MLEs in the PHN($\alpha = 10, \sigma = 50$) model under different scenarios based on 10,000 replicates.

1.3. PPE distribution

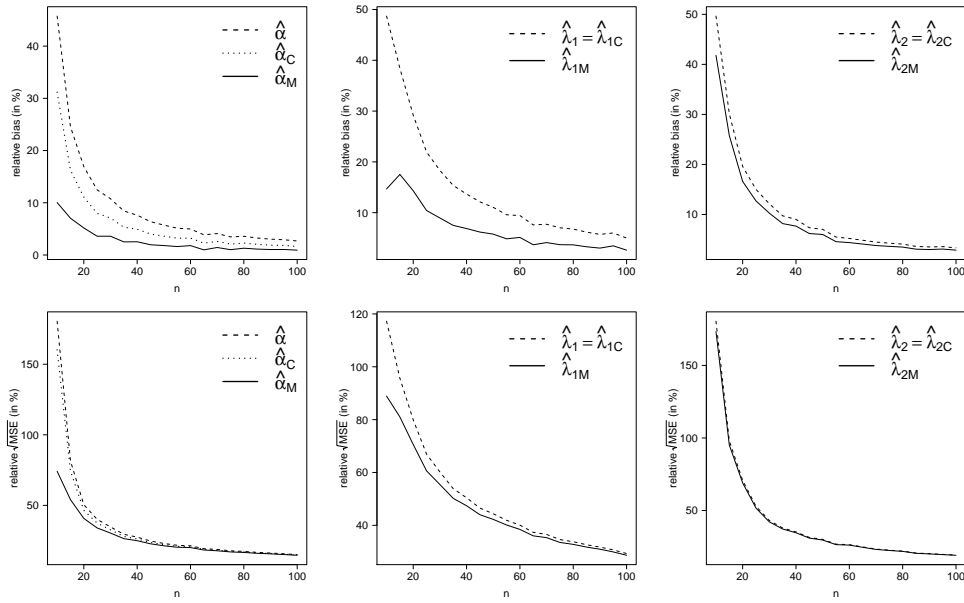


Figure 35: Estimated bias and root MSE for the MLEs and the modified MLEs in the PPE($\alpha = 0.5, \lambda_1 = 0.045, \lambda_2 = 1$) model under different scenarios based on 10,000 replicates.

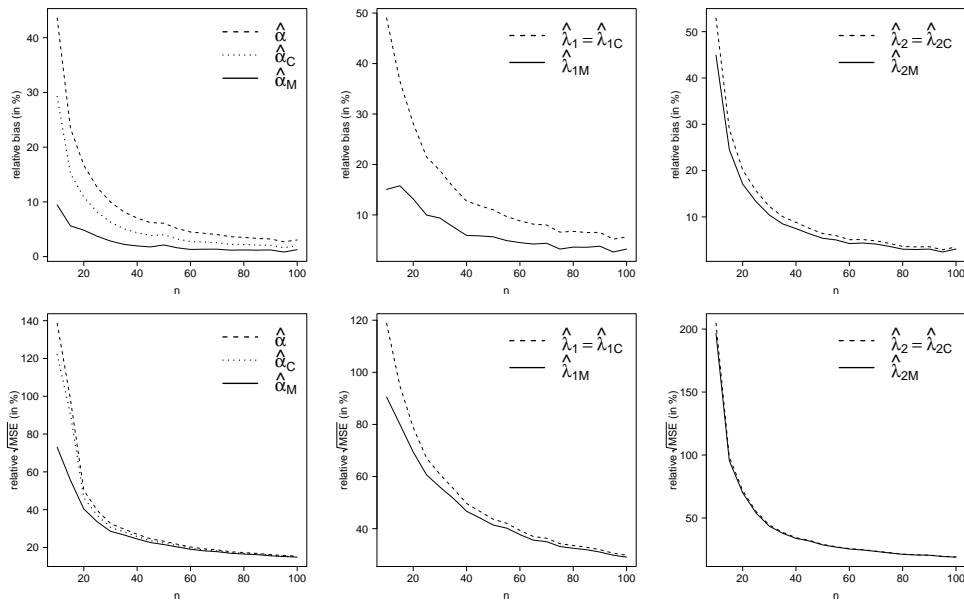


Figure 36: Estimated bias and root MSE for the MLEs and the modified MLEs in the PPE($\alpha = 0.5, \lambda_1 = 0.111, \lambda_2 = 1$) model under different scenarios based on 10,000 replicates.

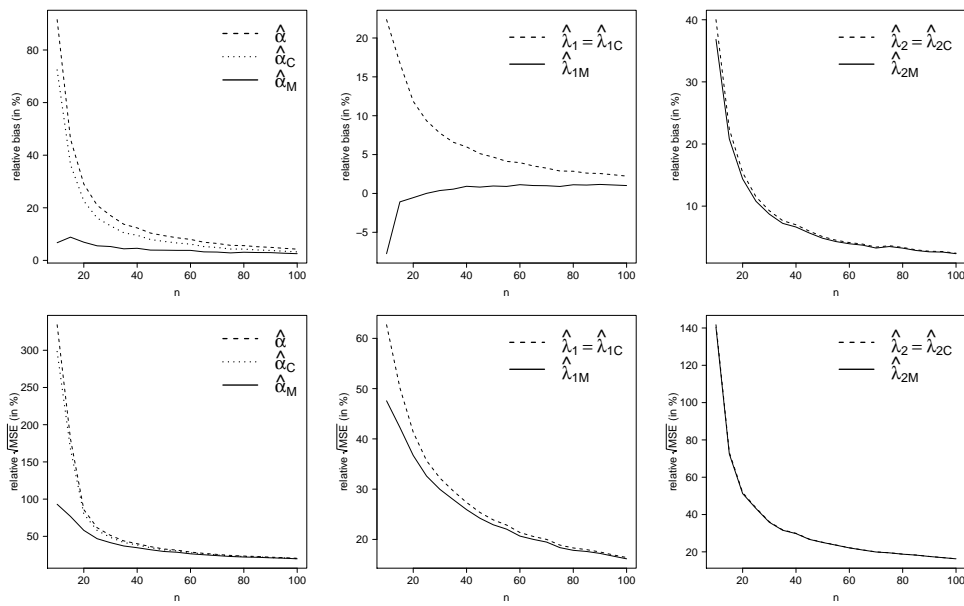


Figure 37: Estimated bias and root MSE for the MLEs and the modified MLEs in the PPE($\alpha = 2, \lambda_1 = 0.149, \lambda_2 = 1$) model under different scenarios based on 10,000 replicates.

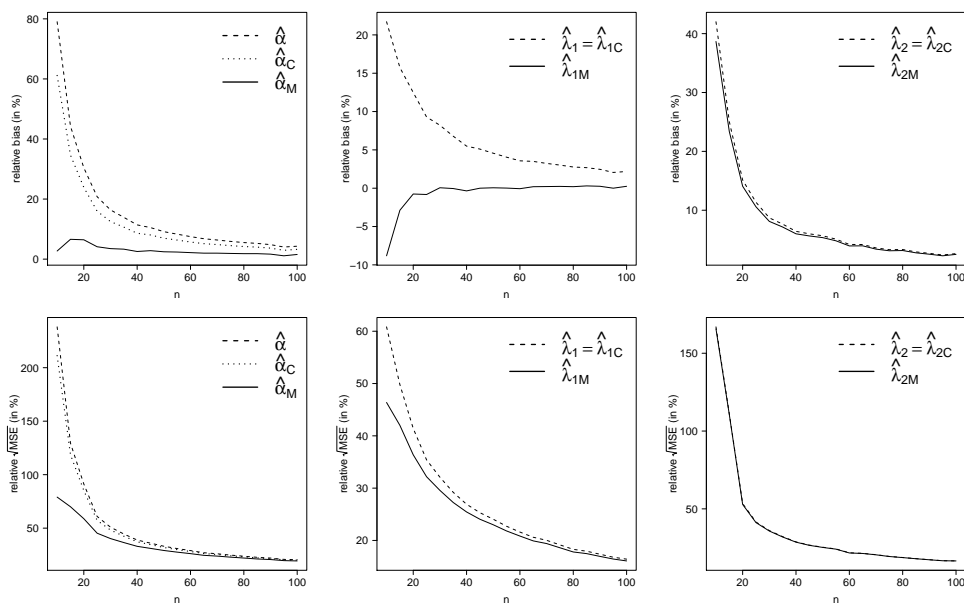


Figure 38: Estimated bias and root MSE for the MLEs and the modified MLEs in the PPE($\alpha = 2, \lambda_1 = 0.372, \lambda_2 = 1$) model under different scenarios based on 10,000 replicates.

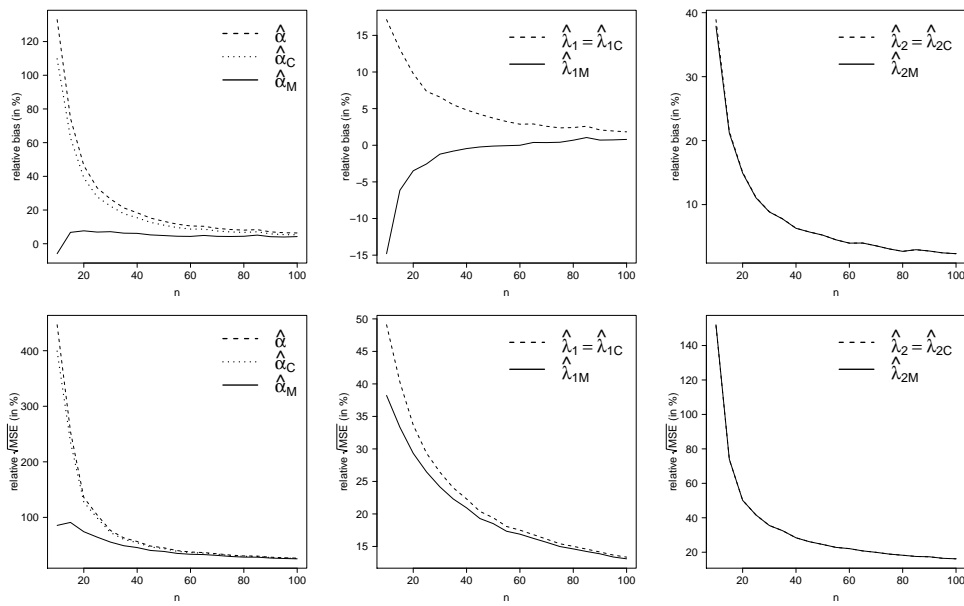


Figure 39: Estimated bias and root MSE for the MLEs and the modified MLEs in the PPE($\alpha = 5, \lambda_1 = 0.233, \lambda_2 = 1$) model under different scenarios based on 10,000 replicates.

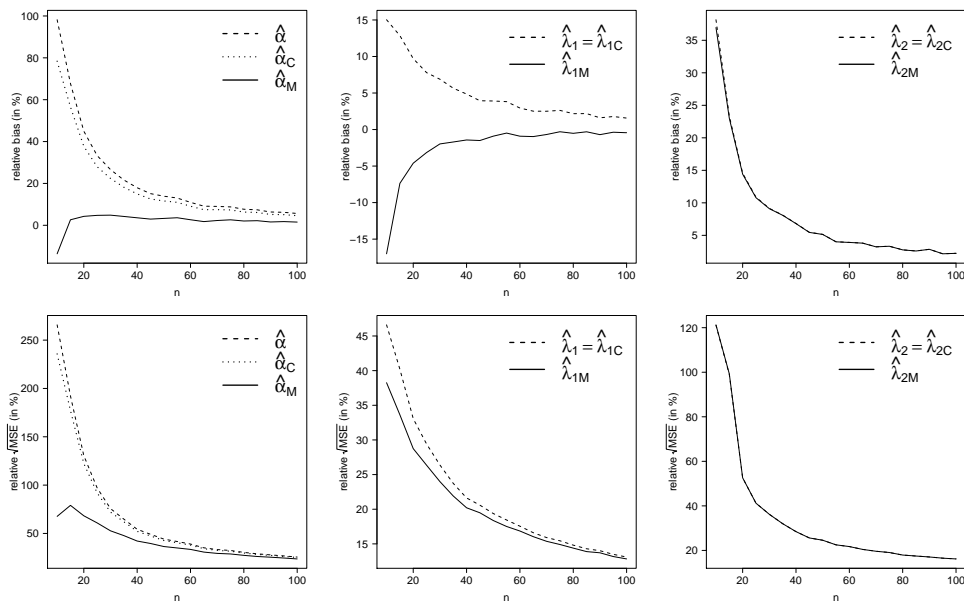


Figure 40: Estimated bias and root MSE for the MLEs and the modified MLEs in the PPE($\alpha = 5, \lambda_1 = 0.583, \lambda_2 = 1$) model under different scenarios based on 10,000 replicates.

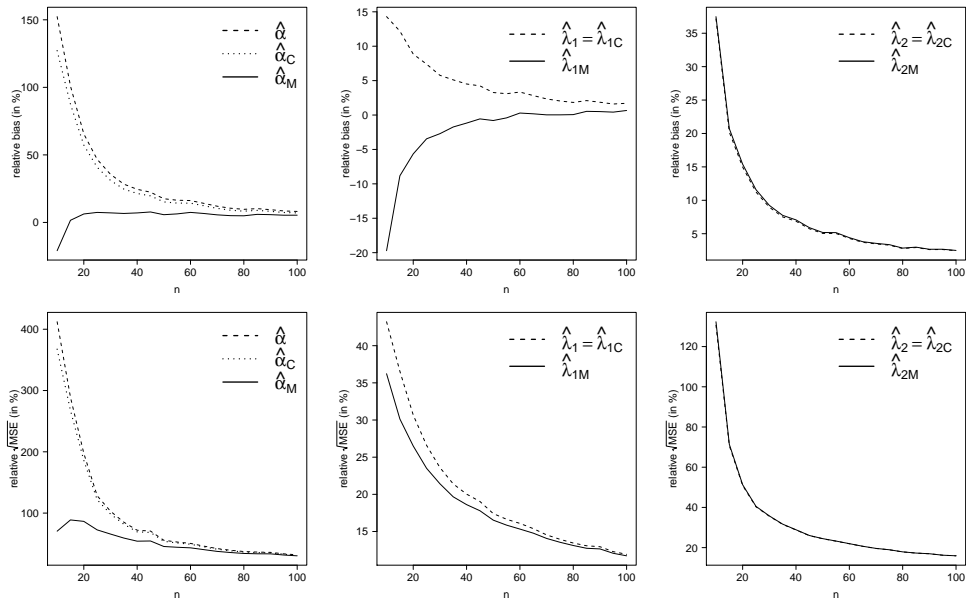


Figure 41: Estimated bias and root MSE for the MLEs and the modified MLEs in the PPE($\alpha = 10, \lambda_1 = 0.300, \lambda_2 = 1$) model under different scenarios based on 10,000 replicates.

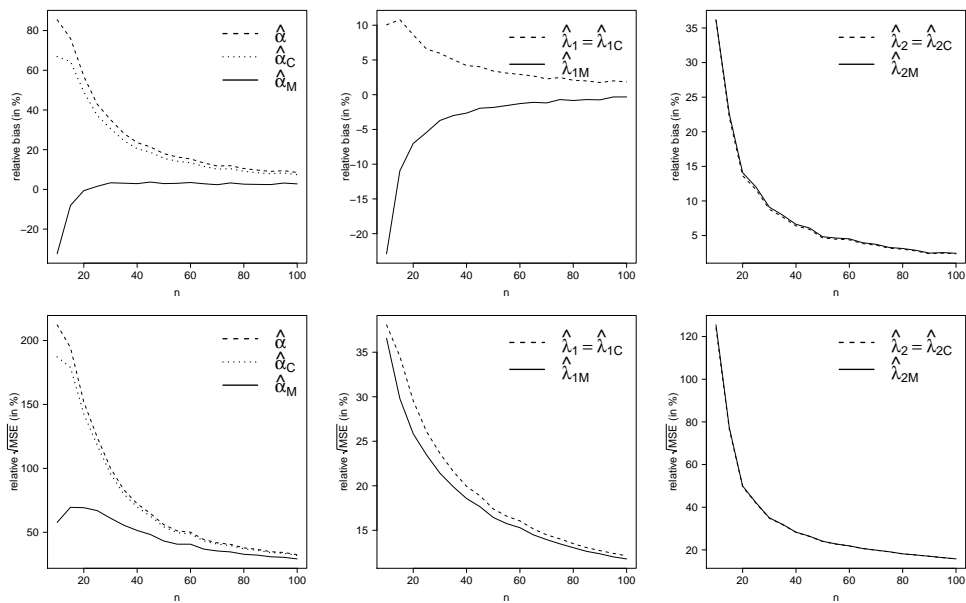


Figure 42: Estimated bias and root MSE for the MLEs and the modified MLEs in the PPE($\alpha = 10, \lambda_1 = 0.749, \lambda_2 = 1$) model under different scenarios based on 10,000 replicates.

2. ADDITIONAL APPLICATIONS

In this section, we provide additional real data applications for models belonging to the $P_f(\alpha)$ class of distributions.

2.1. Additional Illustration for the PHN distribution

The real data set analysis use a data set previously analyzed in Birnbaum and Saunders [1, 2]. It reports the lifetimes of 6061-T6 aluminium pieces (measured in cycles of 10^{-3}) cut in parallel with the direction of rotation, oscillating at the rate of 18 cycles/s at maximum pressure 31,000 psi. The total sample size was 101 units. The data set was analyzed in Gómez and Bolfarine [3] using the PHN model. The MLEs and the modified MLEs for this model are presented in Table 1.

In this example, the confidence interval for α provided by $\hat{\alpha}_M$ is more precise given that it is shorter than $\hat{\alpha}$; the two alternatives present confidence intervals for λ of similar length. Finally, Figure 43a shows the histogram of the data and the estimated density function for both estimates.

Table 1: MLEs and modified MLEs for the PHN model in the Aluminium Pieces data set.

Parameter	$\hat{\sigma}$	$\hat{\alpha}$	$\hat{\sigma}_M$	$\hat{\alpha}_M$
Estimate	55.0906	40.6390	55.6276	38.2748
s.e.	2.3742	9.9366	2.3722	9.1140
95% C.I.	(50.4372 ; 59.7440)	(21.1632 ; 60.1147)	(50.9781 ; 60.2771)	(22.7754 ; 58.5025)

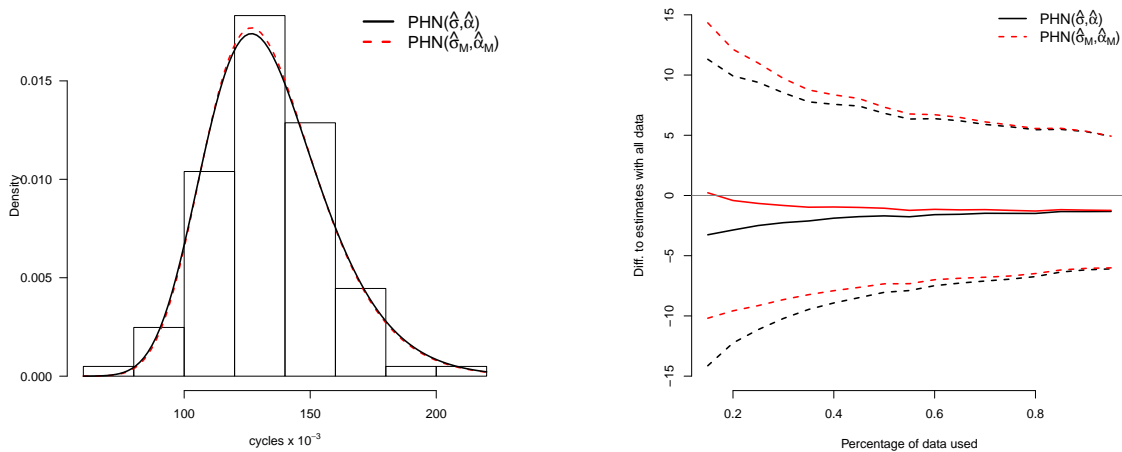


Figure 43: Comparisons of the ordinary and modified MLEs in the Aluminium Pieces data set. Left panel: Histogram for the PHN model and respective density estimate for each proposal. Right panel: Estimated bias (solid line) via 10,000 bootstrap samples considering only a percentage of the data, with estimated 95% confidence interval (dashed line).

Comparison between the estimated densities plotted, together with the histogram, does not show a great difference between results obtained by the ordinary and the modified MLE. This is probably due to the sample size, given that parameter estimation is based on 101 units. If we consider the possibility of not observing all of these points, we could also compare the performance of these two estimators for α . By selecting bootstrap samples with sample size equal to just a percentage of these 101 units, we are able to estimate the bias for each estimator considering the possible non-availability of all data points. The results are shown in Figure 43b, for percentages varying from 0.15 to 0.95, as we report the difference between the estimate obtained with all points as well as that obtained with only part of the data. On one hand, we see that the modified estimator has an almost constant bias for all percentages considered; on the other, the ordinary MLE shows an increasing bias when we start to consider smaller percentages of data availability. This is a further confirmation that the modified MLE should always be preferred in this class of models.

2.2. Additional Illustration for the PBS distribution

For this application, we consider the biaxial fatigue data which was presented by Rieck and Nedelman [6] and then reanalyzed by Martínez-Flórez *et al.* [5]. Although we did not include this example in the simulation studies, we decided to include it using the PBS model to further demonstrate the effectiveness of our modified MLE for the shape parameter in the class of power models. Just as a reminder, the cdf for the Birnbaum-Saunders distribution can be written as

$$F(x; \lambda, \beta) = \Phi[\xi(x/\beta)/\lambda],$$

where $\Phi(\cdot)$ is the cdf of the normal distribution and $\xi(t) = t^{1/2} - t^{-1/2}$. The PBS distribution is then obtained making $G(x; \lambda, \beta, \alpha) = [F(x; \lambda, \beta)]^\alpha$.

Our variable of interest here is the logarithm of the number of cycles to failure, in a set of 46 observations. Table 2 shows the ordinary, corrected and modified MLEs for the PBS distribution in this data set. In spite of the great differences in the scale of the estimates for β and α , the left side of Figure 44 shows that the modified method also gives a good approximation of the data. The modified method presents narrower intervals for the confidence interval of the estimates. Given the different scales, we present an estimate of the relative bias, based on 10,000 bootstrap samples. We removed from the samples those cases where the estimation method crashed, or where the estimates obtained differed too widely from the initial estimates presented in Table 2. The results presented on the right side of Figure 44 show that the estimates obtained from the modified method are far more stable than those obtained by the ordinary method and the Cox-Snell method. This result is visible for all parameters. In particular, it can be seen that for α , zero is outside the limits of the boxplots. Actually this value is classified as an outlier for these bootstrap samples, but outliers were removed from the plot to ease visualization. What this application shows us is that the modified estimators are extremely reliable, with little variation given this resampling scenario; this, is one more argument in favour of this estimation method. Another explanation for the great variation given by the ordinary and Cox-Snell estimates might be problems in the maximization of the likelihood, which are discussed for the Birnbaum-Sanders distribution in Lemonte *et al.* [4]. This could be a topic for further investigation, but we will not pursue it here.

Table 2: Ordinary, corrected and modified MLEs for the PPE model in failure time data set.

Parameter	Estimate	95% C.I.
$\hat{\lambda}$	6.0644	(5.7800 ; 8.7600)
$\hat{\beta}$	0.1660	(0.0260 ; 0.1800)
$\hat{\alpha}$	1.2502	(0.0125 ; 1.8100)
$\hat{\lambda}_C$	6.0644	(5.7800 ; 8.7600)
$\hat{\beta}_C$	0.1660	(0.0260 ; 0.1800)
$\hat{\alpha}_C$	1.2229	(0.0122 ; 1.7700)
$\hat{\lambda}_M$	8.7572	(8.1800 ; 9.0100)
$\hat{\beta}_M$	0.0087	(0.0084 ; 0.0091)
$\hat{\alpha}_M$	0.0011	(0.0009 ; 0.0016)

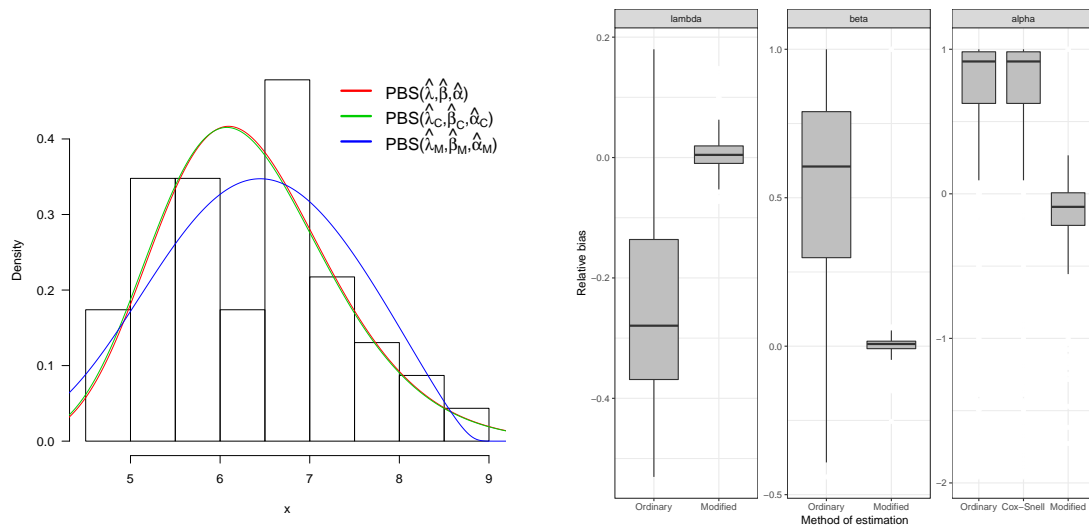


Figure 44: (Left side) Density comparisons based on MLEs, corrected MLEs and modified MLEs for the biaxial data set. (Right side) Boxplot of relative bias for each parameter for MLEs, corrected MLEs and modified MLEs.

REFERENCES

- [1] BIRNBAUM, Z.W. and SAUNDERS, S.C. (1969a). A new family of life distributions, *Journal of Applied Probability*, **6**, 319–327.
- [2] BIRNBAUM, Z.W. and SAUNDERS, S.C. (1969b). Estimation for a family of life distributions with applications to fatigue, *Journal of Applied Probability*, **6**, 328–347.
- [3] GÓMEZ, Y.M. and BOLFARINE, H. (2015). Likelihood-based inference for the power half-normal distribution, *Journal of Statistical Theory and Applications*, **14**, 383–398.
- [4] LEMONTE, A. (2007). Improved statistical inference for the two-parameter Birnbaum-Saunders distribution, *Computational Statistics & Data Analysis*, **51**, 4656–4681.
- [5] MARTÍNEZ-FLÓREZ, G.; BOLFARINE, H. and GÓMEZ, H.W. (2017). The log-linear Birnbaum-Saunders power model, *Methodology and Computing in Applied Probability*, **19**, 913–933.
- [6] RIECK, J.R. and NEDELMAN, J.R. (1991). A log-linear model for the Birnbaum-Saunders distribution, *Technometrics*, **33**, 51–60.